

Proxydetection of the impact distance of trees on crops: An indicator of the Land Equivalent Ratio?

Yélognissè Agbohessou, Alain Audebert, Adama Ndour, Louise Leroux, Christophe Jourdan, Cathy Clermont-Dauphin, Sidy Sow, Caroline Pierre, Simon Taugourdeau, Mame Sokhna Sarr, et al.

To cite this version:

Yélognissè Agbohessou, Alain Audebert, Adama Ndour, Louise Leroux, Christophe Jourdan, et al.. Proxydetection of the impact distance of trees on crops: An indicator of the Land Equivalent Ratio?. Agriculture, Ecosystems & Environment, 2025, 394, pp.109918. ⟨10.1016/j.agee.2025.109918⟩. ⟨hal-05223603⟩

HAL Id: hal-05223603

https://hal.inrae.fr/hal-05223603v1

Submitted on 26 Aug 2025

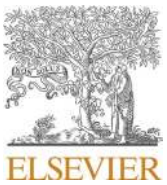
HAL is a multi-disciplinary open access archive for the deposit and dissemination of scientific research documents, whether they are published or not. The documents may come from teaching and research institutions in France or abroad, or from public or private research centers.

L'archive ouverte pluridisciplinaire **HAL**, est destinée au dépôt et à la diffusion de documents scientifiques de niveau recherche, publiés ou non, émanant des établissements d'enseignement et de recherche français ou étrangers, des laboratoires publics ou privés.



Distributed under a Creative Commons CC BY 4.0 - Attribution - International License

Agriculture, Ecosystems and Environment 394 (2025) 109918



Contents lists available at ScienceDirect

Agriculture, Ecosystems and Environment

journal homepage: www.elsevier.com/locate/agee



Proxydetection of the impact distance of trees on crops: An indicator of the Land Equivalent Ratio?

Yélognissè Agbohessou [a,b,*], Alain Audebert [c,d], Adama Ndour [e], Louise Leroux [b,f,g], Christophe Jourdan [h,i], Cathy Clermont-Dauphin [i,j], Sidy Sow [j,k,l], Caroline Pierre [m], Simon Taugourdeau [n,o], Mame Sokhna Sarr [l], Sekouna Diatta [p], Diaminatou Sanogo [l], Josiane Seghieri [i], Guerric le Maire [h,i], Rémi Vezy [q,r], Daniel Fonceka [c,d], Olivier Roupsard [h,i,j]

[a] CIRAD, UPR AIDA, Montpellier F-34398, France
[b] AIDA, Univ Montpellier, CIRAD, Montpellier, France
[c] CIRAD, UMR AGAP Institut, Montpellier, France
[d] UMR AGAP Institut, Univ Montpellier, CIRAD, INRAE, Institut Agro, Montpellier, France
[e] CIMMYT, Addis Ababa, Ethiopia
[f] CIRAD, UPR AIDA, Nairobi, Kenya
[g] IITA, ICIPE Campus, Nairobi, Kenya
[h] CIRAD, UMR Eco&Sols, Montpellier F-34398, France
[i] Eco&Sols, Univ Montpellier, CIRAD, INRA, IRD, Montpellier SupAgro, Montpellier 34000, France
[j] LMI IESOL, Centre IRD-ISRA de Bel Air, Dakar, Senegal
[k] UGB, Saint-Louis, Senegal
[l] CNRF, ISRA, Dakar, Senegal
[m] IEES-Paris, CNRS, Sorbonne Université, Université Paris Est Créteil, Université de Paris, INRAE, France
[n] UMR SELMET, Univ Montpellier, CIRAD, INRA, Institut Agro, Montpellier, France
[o] UMR SELMET, CIRAD, Campus de Baillarguet, Montpellier 34398, France
[p] UCAD, Dakar, Senegal
[q] CIRAD, UMR AMAP, Montpellier F-34398, France
[r] AMAP, Univ Montpellier, CIRAD, CNRS, INRAE, IRD, Montpellier, France

ARTICLE INFO

Keywords:
Faidherbia albida
Distance of influence
Crops
Land Equivalent Ratio
Spectral indices
Geostatistics

ABSTRACT

Faidherbia albida is known to affect the yield of various crops, typically in a pattern where the impact decreases with increasing distance from the tree. While several studies have investigated the spatial extent of this effect, limited research has explored how this distance varies across different crops or its relationship with crop yield and the Land Equivalent Ratio. In this study, we used a geostatistical approach combined with multispectral UAV (Unmanned Aerial Vehicle) imagery to address these gaps in understanding. The results showed that, in contrast to its tripling effect on millet yield, *F. albida* does not have a significant impact on groundnut pod yield, it only improves its haulm yield under its crown by about 50 %. The geostatistical analysis showed that *F. albida* affects the groundnut crop up to 9.8-m, compared to 18-m for millet. Yield upscaling from subplots to the whole plot was achieved with an error of 8 % for groundnut pod yield and 13 % for haulm yield. Groundnut's partial Land Equivalent Ratio (LERcp) was 1.02 for pod yield and 1.05 for haulm yield, which was lower than the LERcp for millet. We concluded that the distance at which agroforestry trees influence crops is a reliable predictor of their effect on yield and Land Equivalent Ratio. This approach offers a promising tool for future agroforestry studies, potentially guiding crop management strategies in agroforestry systems.

* Corresponding author at: CIRAD, UPR AIDA, Montpellier F-34398, France.
E-mail address: fredi.agbohessou@cirad.fr (Y. Agbohessou).

https://doi.org/10.1016/j.agee.2025.109918
Received 5 February 2025; Received in revised form 14 June 2025; Accepted 14 August 2025
Available online 16 August 2025
0167-8809/© 2025 The Authors. Published by Elsevier B.V. This is an open access article under the CC BY license (http://creativecommons.org/licenses/by/4.0/).

1. Introduction

The 2023 global hunger assessment reveals that progress toward ending hunger remains insufficient, with Africa continuing to bear the brunt of this crisis (FAO et al., 2024). This highlights the urgent need for action in the region. In Sub-Saharan Africa, despite recent advances, many nations still face significant food insecurity challenges (Wudil et al., 2022). Since 2000, the region has achieved significant agricultural growth. However, this growth has primarily relied on the expansion of cropped areas rather than improvements in productivity (Jayne et al., 2021). This trend raises a critical question: how can Sub-Saharan Africa transition to more productive and sustainable farming systems to meet its rising food demand? Agroforestry systems represent a potential pathway to address this challenge in the region.

Several authors have proposed integrating trees into cropping systems and adopting agroforestry practices as a holistic approach to address interconnected challenges related to food security, climate change, energy, land management, and water resources in Sub-Saharan Africa (Elagib and Al-Saidi, 2020; Mbow et al., 2014). Agroforestry systems have actually demonstrated significant potential to enhance the productivity of smallholder crops, particularly in arid regions and nutrient-deficient soils (Clermont-Dauphin et al., 2023; Roupsard et al., 2020). Trees can enhance soil nutrient dynamics by improving nutrient availability, reducing losses, and boosting soil quality, which can benefit crop yields (Sida et al., 2019; Yengwe et al., 2018). However, excessive tree density or size may lead to competition with crops for resources, potentially lowering yields (Karlson et al., 2023).

Effective tree-crop pairing in agroforestry requires considering species' phenology, physiology and density to minimize competition and maximize benefits. In this context, *Faidherbia albida (F. albida)* is particularly well-suited for semi-arid systems due to its unique reverse phenology, *i.e.* shedding leaves during the rainy season, when crops grow. *F. albida* plays a key role in agricultural lands, contributing to improve microclimate, soil fertility, nutrient cycling, and crop yield (Dilla et al., 2018; Sida et al., 2018). Agroforestry systems with *F. albida* often outperform monocultures, as reflected by the land-equivalent-ratio (LER), which compares the land needed to achieve similar production under separate management (Mead and Willey, 1980). While *F. albida* provides long-term ecosystem services (Leroux et al., 2022), crop yield (grain, haulm/fodder) holds greater immediate value for farmers, making the crop-specific LER (LERcp) particularly important. In areas with low tree density, a subplot far enough from any tree can serve as a practical reference for estimating crop LER without tree influence.

The distance at which trees influence the crop depends on the configuration of the agroforestry system (the tree species, the crop and the tree species density). Estimating this influence requires a methodology that accounts for the heterogeneity introduced by trees in agroforestry systems, while reducing labor intensity (Roupsard et al., 2020). The development of digital sensors, the democratization of remote sensing techniques (Tang and Shao, 2015), and the emergence of Unmanned Aerial Vehicles (UAVs) of different shapes, sizes and functions over the past decades (Colomina and Molina, 2014) have allowed new studies to revisit this issue (Leroux et al., 2020; Roupsard et al., 2020).

Recent studies have used remote sensing to assess the influence of *F. albida* on crop performance. Roupsard et al. (2020) combined UAV multispectral imagery and geostatistics to estimate *F. albida* influence on millet yield. Diack et al. (2024) and Leroux et al. (2020) extended similar approaches using UAV and satellite imagery to estimate millet fractional cover and yields at broader scales. These methods show promise for upscaling yield estimates and understanding tree-crop interactions. Moreover, the UAV multispectral imagery and geostatistical-based approach is scalable and practical for broader agroecological applications. Further development is needed to extend this approach to other important crops, such as groundnut, a nitrogen-fixing and key agricultural commodity in Senegal that plays a vital role in the rural economy (Noba et al., 2014). Groundnut provides both marketable pods and valuable fodder in the form of haulms (leaves and stems). Using multiple UAV images throughout the growing season, rather than a single image at harvest, may better capture temporal changes in spectral indices that reflect dynamic shifts in crop and tree phenology. This can improve correlations between plant functional traits and spectral indices, while also enabling a more accurate, spatially explicit, and temporally detailed assessment of plant performance and variability across the field (Diack et al., 2024).

In the present study, we built upon prior research study by Roupsard et al. (2020) to investigate how *F. albida* affects crops performance in agroforestry systems. We hypothesized that: (i) crop performance improves under the canopy due to a balance between positive effects and competition; (ii) integrating multi-temporal imagery enables more accurate prediction of key crop traits; and (iii) a wider zone of positive tree impact would correspond to higher yield and greater LER in agroforestry systems. To test these hypotheses, we addressed the following research questions: (i) How does groundnut crop perform according to its distance to *F. albida*? (ii) Can we improve crop traits predictions using several MS images throughout the crop cycle? (iii) How does the distance of influence of agroforestry trees correlate with crop yield and the Land Equivalent Ratio (LER)?

2. Materials and methods

2.1. Study area

The study area is located at the well-instrumented "Faidherbia-Flux" site (https://lped.info/wikiObsSN/?Faidherbia-Flux), located in the Niakhar/Sob region, a Serer locality within Senegal's groundnut basin (coordinates: N: 14°29′44.916″; W: 16°27′12.851″). This site is a typical agroforestry park characterized by a sparse tree population (6.8 trees ha^{-1} and a canopy cover of 5.14 %), predominantly consisting of *Faidherbia albida*, and is part of the Niakhar Observatory (Observatoire Population Santé Environnement (OPSE): https://lped.info/wikiObsSN/?HomePage) (Roupsard et al., 2020). The understorey consists of a crop mosaic, including groundnut, millet, watermelon, cowpea, and fallow land (Fig. 1A and 1B). Agriculture and livestock farming are central to the livelihoods of the local population. In this region, millet serves primarily as a staple crop and is cultivated in rotation with groundnut, which is grown as a cash crop.

The climate is Sudanian-Sahelian, with a unimodal rainfall pattern, featuring a distinct rainy season from June to October. The region experiences relatively stable temperatures throughout the year. Notably, annual rainfall varies significantly from year to year, both temporally and spatially (Delaunay, 2017). From 2018 to 2022, the average annual precipitation was 574 mm (range: 454–822 mm), and the average annual air temperature was 27.62 °C (range: 27–28 °C). The soils are sandy (0–50 cm layer: 82.1 % sand; 8.9 % clay; soil pH approx. 6.52) and very poor in nutrients (Siegwart et al., 2023).

2.2. In situ data collection: crop sampling, plot management, laboratory analyses and whole plot yield estimation

Two whole plots (> = 1 ha each) were monitored in 2019 (Fig. 1A and 1B), under annual crop rotation (groundnut, i.e. *Arachis hypogaea var. 55–437 (short-cycle variety of 90 days)*; pearl millet, i.e. *Pennisetum glaucum var. Souna*) and located less than 300 m apart. Groundnut was cropped in Plot A (Fig. 1A, previously with millet in 2018 (Roupsard et al., 2020)) and millet in Plot B (Fig. 1B, previously with groundnut in 2018).

Experiment 1 (exp 1) was carried out in plot A (Fig. 1A) only (on groundnut only), while experiment 2 (exp 2) was performed in both plots (Fig. 1A and 1B). In Fig. 1, the plot B appears to be greener than the plot A. This observation is actually due to the difference in growth stages on the date of the flight, as confirmed by Fig. 3. Experiments 1 and 2 are

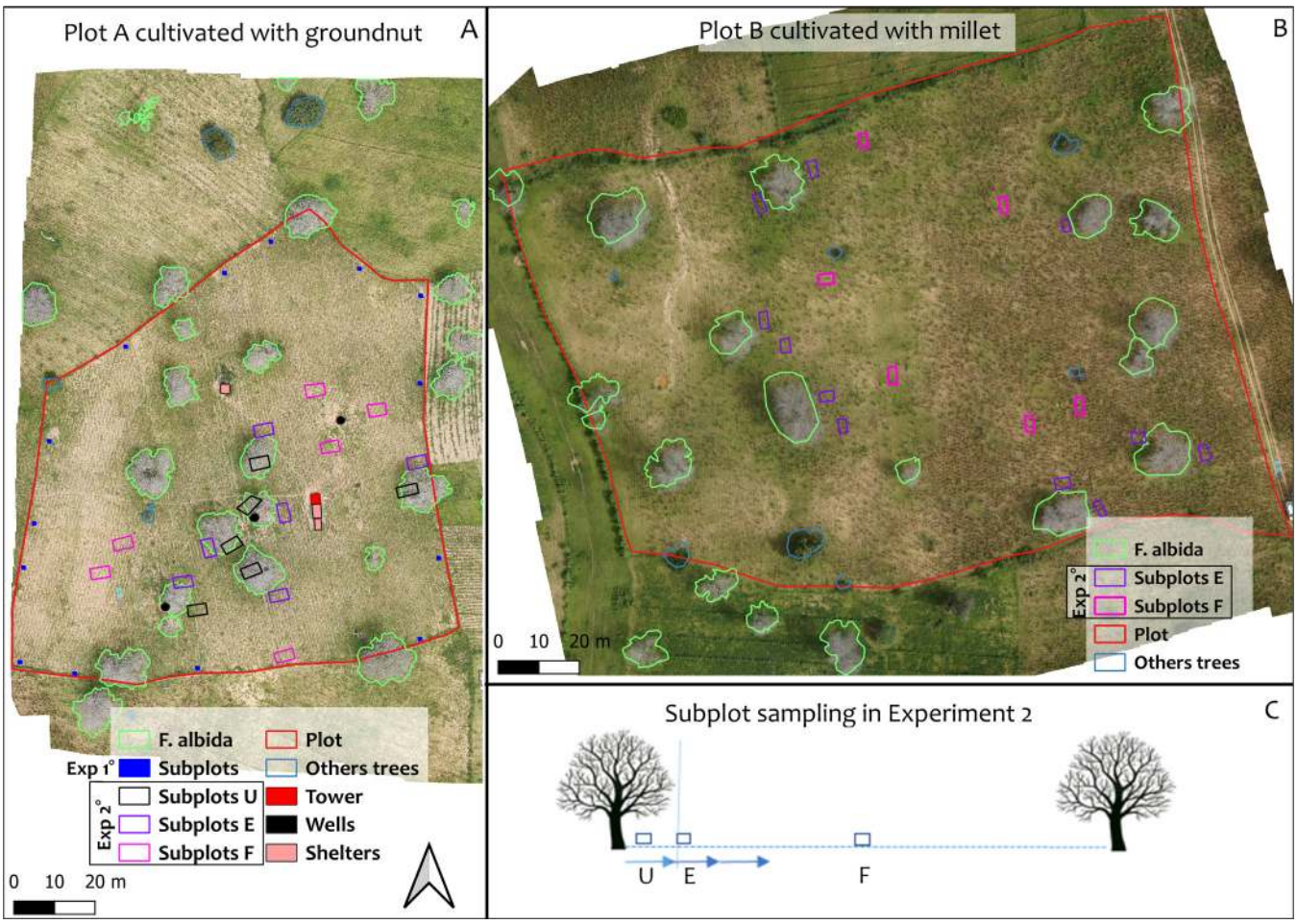


Fig. 1. Experimental set up and subplot locations for Experiments 1 and 2 in plots A and B (2019). A/ Plot A (groundnut crop, image date: 2019-10-29). Subplots for Experiment 1 are shown as small blue cells located at the edges of the plot. Subplots for Experiment 2 are represented by larger rectangular cells labeled U, E, and F, distributed within the plot. B/ Plot B (millet crop, image date: 2019-10-17). Subplots for Experiment 2 on this plot are shown by rectangular cells labeled E and F. C/ Sampling scheme for Experiment 2 subplots relative to a *F. albida tree: "U (Under)": Subplot directly beneath the tree crown (not visible in drone imagery). "E (Edge)": Subplot at the edge of the tree crown. "F (Far)": Subplot located more than 25 m away from the tree trunk, outside the crown area. Each distance category includes 6 replicate subplots (~ 15 m² each), totaling 18 subplots per plot.*

described in detail in the following sections.

2.2.1. Monitoring of groundnut biomass using periodic destructive measurements (Exp 1)

Groundnut plants were destructively sampled twice a week throughout the crop cycle (from 2019/07/27 to 2019/11/09) in replicated subplots per collection date of 1 m^2 each, randomly selected at the edge of the "Plot A" to minimize impact on the whole plot estimations. Groundnut plant height was measured first, then pod, leaf, stem root and flower were harvested separately on each subplot. The different plant organs were wrapped in kraft envelopes in the field, then sent to the lab for oven drying and weighing. After drying, the biomass of each plant organ was calculated individually and expressed in grams per square meter, based on the sampled ground area. The average biomass of each organ across the replicated 1 m^2 subplots was then reported for each collection date.

2.2.2. Measurement of groundnut and millet biomass under F. albida (Exp 2)

For all measured variables, we evaluated the effect of the factor "Distance to tree" by establishing subplots of ca. 15 m^2 each at three distinct positions relative to the tree crown: "U (Under the crown)": directly beneath the tree canopy, "E (Edge of the crown)": at the perimeter of the canopy, and "F (Far from the crown)": located more than 25 m away from the tree trunk (Fig. 1C). At each of these positions, 6 replicates were established, totaling 18 subplots per plot. This design was implemented in both plot A and plot B, resulting in a consistent spatial sampling structure. In addition to subplot-level measurements, we also recorded key morphological characteristics of the selected trees including tree height, crown diameter, and girth at breast height.

The number of crop leaves per plant and plant height were measured in each of the 18 subplots once a week on both plots all along the whole crop cycle. Before crops were harvested, fresh leaves were collected on two whole plants, at the outer edge of each subplot. The fresh leaves were scanned (Canon Lide 300), then oven dried and weighed. We measured the leaf area and computed the specific leaf area (SLA) for leaf samples. Using the average of fresh leaves biomass harvested of each corresponding subplot, we calculated the leaf area and leaf area index (LAI) for each subplot.

At the end of the season, all subplots in both plots were harvested. Groundnut (Plot A) was harvested on 2019/11/04, approximately one month after millet (Plot B), which was harvested on 2019/10/21. For millet, we harvested all the ears from each subplot and separated the vegetative biomass into leaves, stems, and roots. Roots were collected from a 5-m-long row within each subplot, and their biomass was subsequently extrapolated to the entire subplot area. For groundnut, a 1 m^2 sub-subplot was established within each 15 m^2 subplot. Groundnut organs (pods, leaves, and stems) were collected separately from both the

15 m^2 subplot and the 1 m^2 sub-subplot. Fresh weights for each organ were measured in the field, after which an excavation (1 m^2 surface area × 0.5 m depth) was made at the location of the sub-subplots to collect any remaining roots after pod harvesting. Roots were sampled separately at depths of 0–10 cm and 20–50 cm, weighed fresh in the field, then dried in an oven and weighed in the lab. Groundnut root biomass was calculated for both the 0–10 cm and 20–50 cm depths, and the total root biomass (excluding pods) was determined for all six subplots.

We assessed the whole-plot yields for both crops (plots A and B). After harvesting the 18 subplots, the farmer and his family harvested all other groundnut plants in the entire plot. The plants were gathered in small heaps, with each heap being counted and weighed in the field. We then used the ratio of the fresh weight of the heap to the dry weight of the pods, to estimate the total dry weight of the pods for the entire plot.

The litter (amount of crop and weeds residues left-over in the field after harvest) was computed for groundnut (roots, weeds) and millet (shoots, roots, weeds). Variables were reported on a dry matter basis and per unit ground area.

2.2.3. Groundnut foliar biomass

Using the dynamics of the number of leaves per groundnut plant all along the cropping season (Exp 1, plot A), we identified the date of the maximum groundnut foliar biomass (2019/10/03), before senescence and leaf shedding. Assuming that the number of leaves per plant was proportional to the leaf biomass per plant, we estimated the maximum leaf biomass in each subplot as the following (Eq. (1)).

$$Leaf\ Dry\ Mass_{\max} = \frac{Leaf\ Dry\ Mass_{harvest} \times Leaf\ Number_{\max}}{Leaf\ Number_{harvest}} \quad (1)$$

This maximum leaf biomass (*Leaf Dry Mass*$_{max}$) corresponds to the peak leaf biomass observed before senescence and leaf shedding. Early signs of leaf spot were observed on groundnut plants prior to leaf drop. Estimating the maximum leaf biomass enables an assessment of the effect of *F. albida* on the potential leaf production before losses (see comparison between maximum leaf biomass and leaf biomass at harvest in Supplementary Fig. A1).

The leaf spot observed is most likely caused by 'black Sigatoka' (*Cercospora arachidicola S. Hori*), a common groundnut foliar disease in Senegal, which typically reaches peak severity around pod maturity (Zongo et al., 2019). However, since we did not quantify the extent of leaf spotting in our subplots during the field campaign, we lacked the necessary data to include this variable as a confounding factor in our statistical analysis.

2.2.4. Soil analysis

A couple of days after sowing (July 2019), 4 soil samples were collected at the outer corners of each subplot at 0–10 cm and 10–30 cm depths using a core sampler. We made 2 composite soil samples per subplot. The total of 36 soil samples (N = 2 samples × 18 subplots) collected were air dried and analyzed in the "Laboratoire des Moyens Analytiques" (LAMA) at "Institut de Recherche pour le Développement" (IRD-Dakar) for soil properties (texture, pH, mineral content, organic content, cation exchange capacity (CEC)).

2.3. UAV data acquisition and processing

2.3.1. UAV characteristics, flights and main processings. The same equipment and process were used to acquire UAV data on both plots (A and B). For plot A (groundnut), we carried out three UAV flights. The first flight (flight 1), before mid-growth season (2019-09-05, 38 days after germination), the second one (flight2), three weeks before harvest (2019-10-17, 80 days after germination) and the last, one week before harvest (2019-10-29, 92 days after germination). The UAV flew at 4.5 m s^{-1} and 50 m above ground, capturing images every second with both RGB (Red, Green, Blue) and multispectral cameras, yielding spatial resolutions of 0.6 cm and 2.7 cm, respectively. Areas beneath tree crowns were not imaged due to flight safety limitations. However, on the plot A, we have also manually taken images of the subplots located under the trees' crown using a camera suspended from a 2.5 m high pole. This allows to compute vegetation indices for the subplots that are under the trees' crown and were not visible when flying the UAV over the whole plot. For "Plot B" (millet), we had two UAV flights, 9 and 2 weeks before harvest, respectively. The characteristics of the UAV system, flight plan, and image processing method are identical to those described in Roupsard et al. (2020) and are detailed extensively in their paper.

2.3.2. Derived vegetation productivity proxies

We used the same method to derive vegetation indices (VIs) for both crops. RGB orthoimages acquired for each plot were used to segment the groundnut and millet under-crops, removing soil and trees in the process. To achieve this, we converted the orthoimages from RGB to HSV color space and performed thresholding operations on the green crops to generate the groundnut and millet masks. Using these masks, we extracted the calibrated reflectances from the NIR, Red, and Green bands, which were then used to calculate the vegetation indices following the equations provided in Table A1. The derived vegetation indices are: Normalized Difference Vegetation Index (NDVI), Green Normalized Difference Vegetation Index (GNDVI), Second Modified Soil-Adjusted Vegetation Index (MSAVI2) and Corrected Transformed Vegetation Index (CTVI).

2.3.3. Method for estimating the sole groundnut vegetation indices (VIs) signals from the total vegetation indices "groundnut + weeds"

Weeds' presence heavily influenced the VI images of the last flight. Only groundnut VIs signals should be used ideally to compute the distance of influence of *F. albida* on groundnut and to estimate groundnut pod and haulm yields. This allows for a more accurate assessment of their contribution to the VI signal. NDVI is sensitive to the chlorophyll content of plants, and its high values (close to 1) are associated with the highest possible green leaf area densities (Rouse et al., 1974). Therefore, we assumed that the total NDVI signal "groundnut + weeds" was proportional to the total aboveground biomass (groundnut haulm + weeds), and similarly for groundnut only NDVI signal being proportional to the groundnut haulm biomass. Based on that assumption, we simply applied the ratio of groundnut haulm biomass to total aboveground biomass on the total NDVI "groundnut + weeds" to estimate the groundnut NDVI in each subplot. At the whole plot level, we used the average ratio. This assumption is mostly valid if the relationship between NDVI and plant biomass is linear, which is the case in our conditions of relatively low LAI (refer to Fig. A2 in the Supplementary materials to observe the linear relationship between total aboveground biomass (groundnut haulm + weed) collected at harvest and the NDVI index from the 3rd UAV flight conducted six days prior to harvest).

2.3.4. Creation of the grid of analysis

Analyses were conducted using R 3.6.1 (R Core Team, 2019) and QGIS 3.4 (QGIS_Development_Team, 2019). Shapefiles were created for whole plots, non-cultivated areas, cultivated areas, and *F. albida* tree crowns. The high-resolution UAV images were aggregated into grids (~5 m^2 for whole plots, ~1 m^2 for subplots), and average NDVI, GNDVI, MSAVI2, and CTVI were calculated for each cell. A distance matrix was generated between grid cells and the nearest *F. albida* tree (k = 1), including trees up to 60 m outside the plot. The final dataset, combining vegetation indices and tree distances, was used for geostatistical analysis.

2.4. Assessment of the distance-decay effect at different scales

To analyze tree effects at the subplot scale, we used one-way ANOVAs when data met homoscedasticity (Bartlett test) and

normality (Shapiro-Wilk test). Otherwise, a Kruskal-Wallis test was applied. Post hoc comparisons were done using Tukey's honestly significant difference test. Statistical significance was assessed using p-values, with a threshold set at $p < 0.05$.

At plot scale, we analyzed the effect of 'distance to tree' (Range parameter) on groundnut and millet using geostatistics in R (R Core Team, 2019). Using attribute data from the geomatics chain and the gstat (Pebesma, 2004) and sp (Bivand et al., 2008) libraries, we plotted semi-variograms of grid cell VIs based on distance to the nearest tree crown centroid (up to 60 m) along four azimuths (N, S, E, W). We noticed that the plot cultivated with millet was anisotropic. We followed each azimuth separately for this plot and maintained the 90° azimuth (East) because millet performed better at the East side of the plot (Fig. 1B). The autofitVariogram function from the automap library (Hiemstra et al., 2009) was used to automatically select the optimal geostatistical model for the spatial data. After evaluating several candidate models for both crop datasets, the 'Ste' model, a parameterization of the Matern model as described by Stein (2012), was found to be the best fit. The Matern model is widely used in spatial statistics to represent spatial correlation structures (Matérn, 1960). The 'Ste' variant incorporates modifications by Stein (2012) to better address specific spatial characteristics, such as non-stationarity and anisotropy, which are common in environmental data.

2.5. Estimation of yield and Land Equivalent Ratio (LER) for crops

To estimate groundnut and millet yields at whole plot scale, multiple linear regression models were tested using groundnut and millet traits as target variables and the different vegetation indices over the UAV flights as independent variables to account for information on vegetation development all over the cropping season. Before building the models, a correlation matrix of the predictor variables was calculated using the *cor ()* function from the caret R package (Kuhn, 2008). The *findCorrelation()* function from the same package was then applied to the matrix with a cutoff value of 0.8 to identify and select highly correlated variables (correlation greater than 0.8). This step helps eliminate redundant variables and reduce multicollinearity, improving the models' stability and interpretability. We then applied stepwise selection to identify the best regression models and used their coefficients to generate yield maps for groundnut pods and haulm at the whole plot scale.

We calculated the LERcp for the groundnut crop alone (for pod and haulm yield) using Eq. (2):

$$LER_{cp} = \frac{Y_i}{Y_s} \quad (2)$$

where, Y_i is the yield in agroforestry and Y_s the yield in monoculture. We divided the yield map into three zones: (i) beneath the tree crown, (ii) between the tree crown and Range boundary, and (iii) beyond the Range. The yield beyond the Range (Ys) was calculated separately. The total yield (Yi) was determined by summing the weighted average yields for each zone, including the area within the Range. We also computed an alternative Yi using pixels below the Range limit. Finally, we compared two LERcp values based on the different Yi options for groundnut pod and haulm yields.

3. Results

3.1. Groundnut and millet growth

3.1.1. Dynamics of groundnut growth (destructive Exp 1)

For groundnut, the growing season lasted about 97 days between the date of germination (2019/07/30) and the harvest date (2019/11/04). Flowering occurred 18 days after germination, on August 17, 2019. The relative importance of organs, in decreasing order of final biomass, was pod, leaf, stem and root (Fig. 2). The biomass produced by the flower was insubstantial as compared to that produced by other organs. An increasing production of pod, root and stem biomass was observed in plants until the 2nd drone flight (2019/10/17, 79 days after germination), then the biomass of these compartments remained globally stable, with variations depending on the subplot. Notably, a significant drop was observed on October 14, although this was not observed in the following measurement. In particular, the pod biomass remained stable between the last two drone flights. Noteworthy, a drastic drop in leaf biomass (approximately 52 %) was observed during the last three weeks

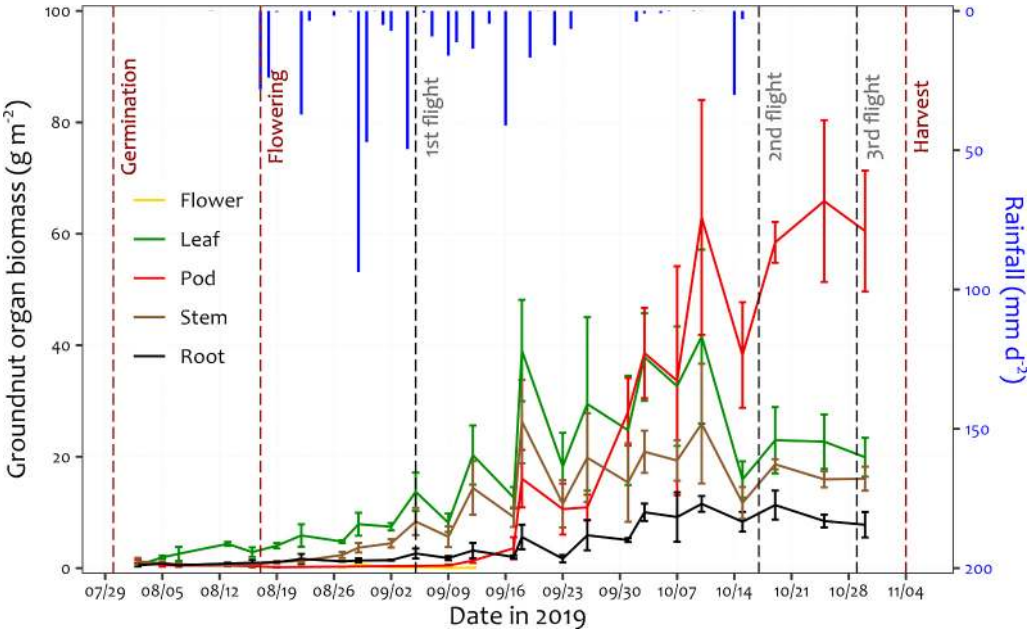


Fig. 2. Time-course of daily precipitation and groundnut biomass per organ in destructive Experiment 1 (see Fig. 1 A), from the sowing date (0 = 2019/07/27) to harvest (2019/10/04, dashed red line). One vertical graduation per week. Error bars are the standard deviations. Leaf shedding (approximately 52 % of leaf biomass) was recorded between week 11 (2019/09/14) and the harvest date (vertical dashed red line). Dashed black lines indicate the drone flights, while vertical dashed red lines indicate the germination date, flowering date, and harvest date, respectively.

before harvest. In addition, the greatest biomass for each plant organ was reached approximately 72 days after germination.

3.1.2. Groundnut and millet growth monitoring: number of leaves and plants height (Exp 2)

In plot A, for all groundnut subplots (U, E, F), leaf number and plant height increased up to the 65th day after germination, with maximum number of leaves per plant of 48 ± 21 and maximum heights of 39 ± 11 cm (in subplots U on 2019/10/03). The plants with the largest number of leaves (Fig. 3a) and also taller (Fig. 3b), were observed under the trees' crown (U). The further from the trees, the fewer leaves plants produce (Fig. 3a) and the shorter the plants (Fig. 3b). Drastic leaf drops of about 79 %, 78 % and 62 % were observed in subplots U, E and F, respectively, during the last three weeks before harvest (Fig. 3a).

Similar results were found in millet (plot B), where plants under the trees' crown presented the largest number of leaves (Fig. 3c) and were taller (Fig. 3d). Fewer leaves were observed for plants further from the tree, but the number of leaves at crown edge (subplots B) was not significantly different from the number of leaves in the subplots F (far from the trees) (Fig. 3c). The further away from the trees, the shorter millet plants become (Fig. 3d). Overall, a leaf drop was observed during the last four weeks before harvest (Fig. 3c) also the time when maximum plant height was achieved.

3.2. Groundnut performance at harvest in subplots according to distance from F. albida trees

The effect of the distance from the *F. albida* tree was not significant neither on the groundnut pod yield ($p = 0.79$) (Fig. 4a), nor on its haulms yield ($p = 0.08$) (Fig. 4b) as measured at harvest. Apart from stem biomass that significantly decreased at distance from *F. albida* trees ($p = 0.035$) (Fig. 4d), no significant difference was observed for other traits such as leaf biomass ($p = 0.41$) (Fig. 4c) and root biomass ($p = 1$) (Fig. 4e). Weed biomass was also not affected ($p = 0.14$) (Fig. 4f). However, at harvest, this lack of significant effects was highly hindered by leaf shedding during the last stages. Therefore, the foliar biomass observed at harvest was recalculated to estimate its status at the time of maximum leaf development. Other foliar biomass-dependent traits such as haulm biomass and LAI were also recalculated. Indeed, the estimated maximum leaf biomass ($p = 0.007$) (Fig. 4g) and the maximum LAI ($p = 0.009$) were significantly reduced at distance from *F. albida*. Twice as much haulm yield was then obtained under tree (S: 146.18 ± 41.49 SD g m^{-2}), as compared to subplots located at 25 m from *F. albida* trunk (H: 69.39 ± 20.74 SD g m^{-2}) (Table 1 and Fig. 4h).

The spectral indices of the first flight were not significantly affected by the distance to *F. albida* (Table 1), but during the last flight when weeds were present, NDVI GNDVI and MSAVI2 (groundnut & weeds) were significantly affected by the distance to *F. albida*. Increasingly strong signals were observed near trees (Table 1, Fig. 5a–c). The performance at harvest in subplots, according to distance from *F. albida* trees, was presented for all measured groundnut traits and the spectral indices obtained from the three UAV flights in the Supplementary material, Table A2.

3.3. Soil nutrient status in subplots according to distance from F. albida trees

The position relative to *F. albida* trees had a significant impact on soil properties, specifically nitrogen (%N), carbon (%C) and organic carbon ($p < 0.05$). Higher levels of %N, %C, and organic carbon were found

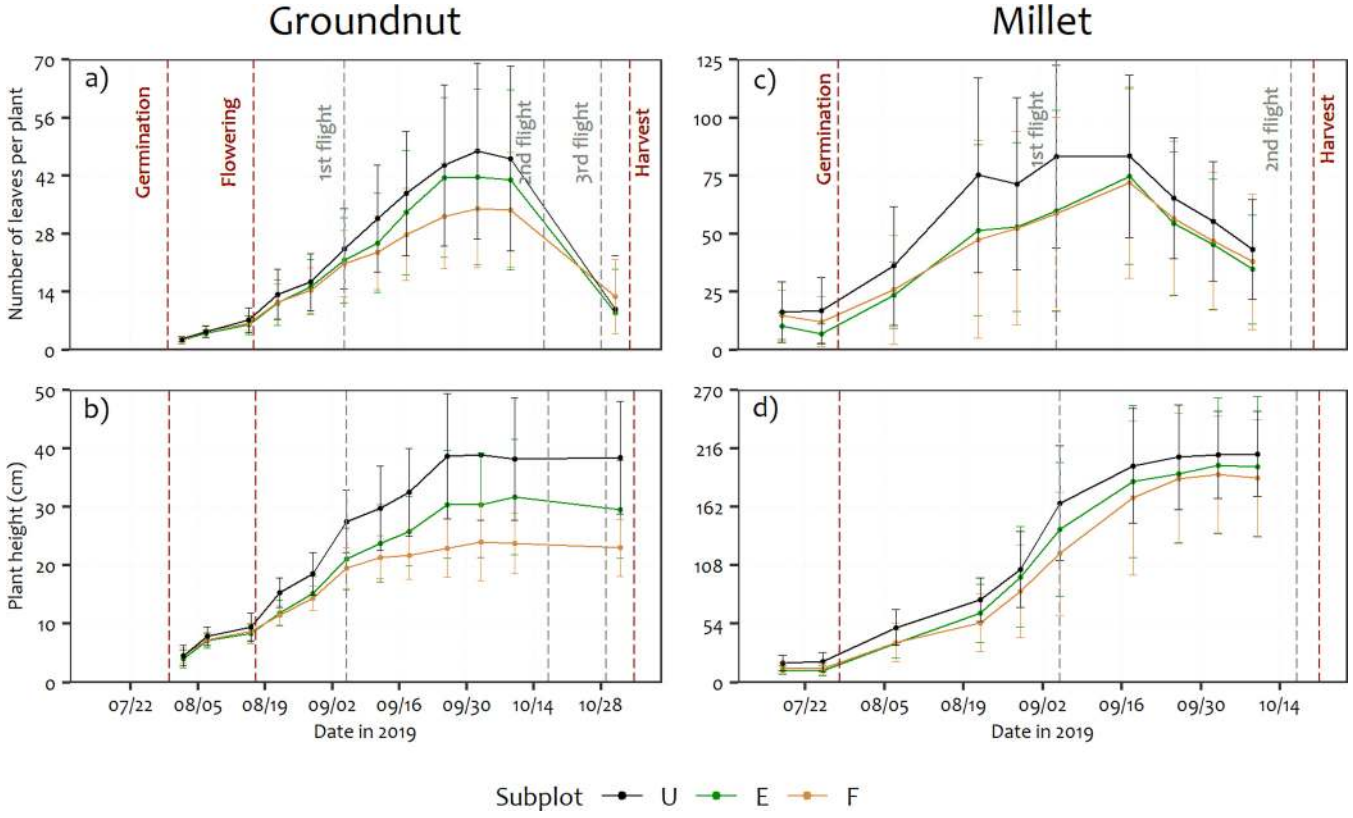


Fig. 3. Time-course of the number of leaves per plant **(a, c) and of plant height (b, d) of groundnut and millet in the subplots of Experiment 2 (see** Fig. 1) until harvest. Vertical graduations represent weeks. Error bars are the standard deviations. Measurements carried out at 3 distances (U, E, F) from the tree ("U": subplots under the tree crown (not visible to the drone), "E": subplots at the edge of the tree crown and "F": subplots far away, outside the tree crown (> 25 m from the trunk)), see Fig. 1C. N= 6 subplot replicates (of ca. 15 m^2 each) per distance to tree. Total number of subplots per plot = 18. Vertical dashed black lines indicate the three drone flights, while vertical dashed red lines indicate the germination date, flowering date, and harvest date.

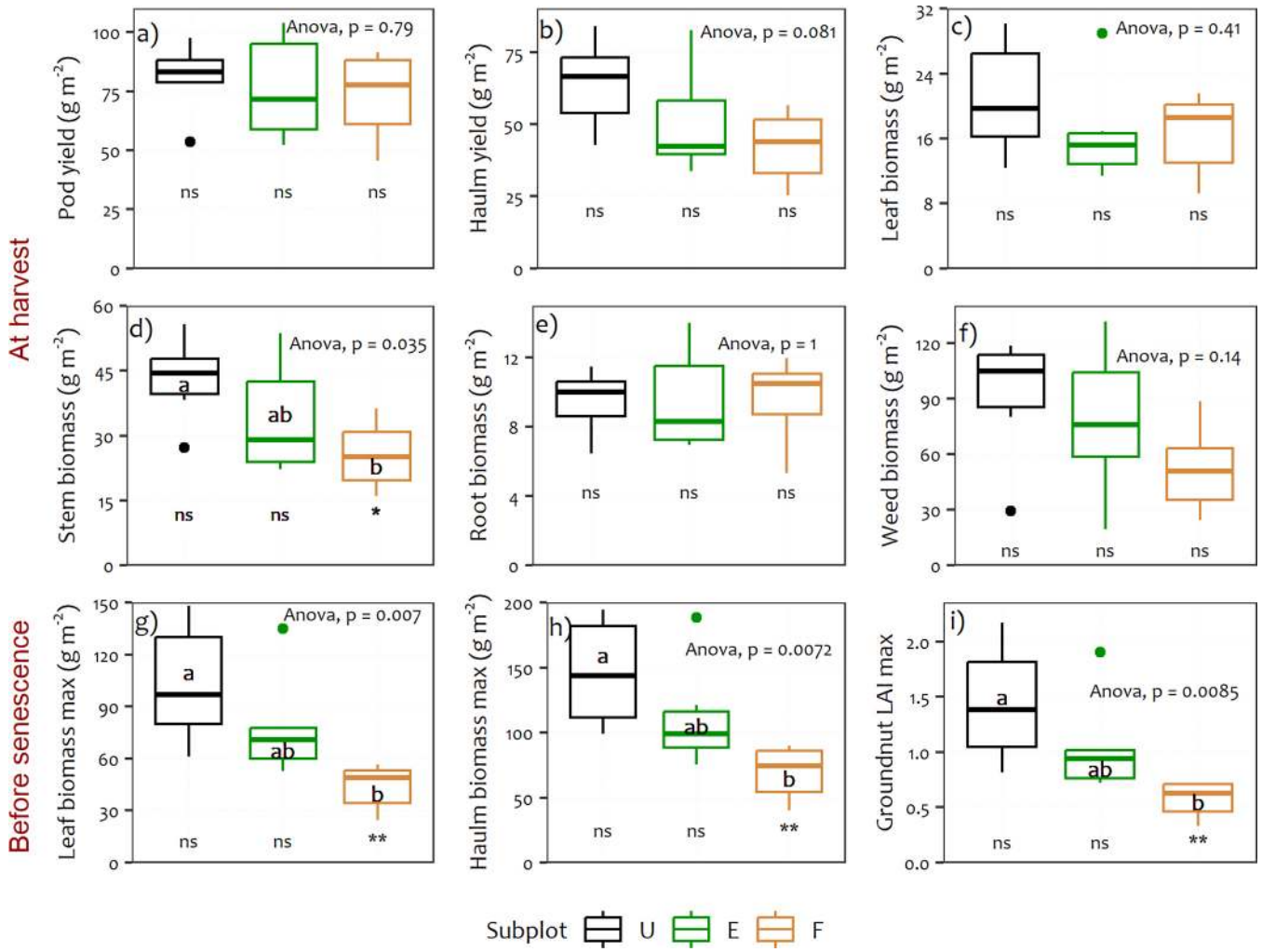


Fig. 4. Effect of the distance to *F. albida on groundnut and weed growth traits in Experiment 2 at harvest (a–f) and before leaf senescence (g–i), i.e. at the maximum of leaf development (according to Experiment 1). Measurements carried out at 3 distances (U, E, F) from the tree ("U": subplots under the tree crown (not visible to the drone), "E": subplots at the edge of the tree crown and "F": subplots far away, outside the tree crown (> 25 m from the trunk)), see* Fig. 1C. N = 6 subplot replicates (of ca. 15 m^{2} each) per distance to tree. Total number of subplots per plot = 18. (ns) Not significant; (**) significant at 0.05; (**); significant at 0.01.

under the tree crown (U) at both 0–10 cm and 10–30 cm depths, compared to the subplot located farther from the tree crowns (F). At the 0–10 cm depth, the values were as follows: under the tree crown (U): %N = 0.03 ± 0.00, %C = 0.39 ± 0.07, compared to the far subplot (F): %N = 0.02 ± 0.00, %C = 0.21 ± 0.04. Similarly, at the 10–30 cm depth, under the tree crown (U): %N = 0.023 ± 0, %C = 0.24 ± 0, compared to the far subplot (F): %N = 0.020 ± 0, %C = 0.20 ± 0.02 (Tab. A3). The difference in soil nutrient properties in both depths was not significant for available P. However, the soil exchange capacity was significantly greater under tree crown (S) at 0–10 cm depth (1.60 ± 0.17 SD) (Tab. A3). The other soil properties such as: pH (H_20 and KCl), C/N and exchangeable cations (Ca, Mg, Na and K) were not affected by the position to *F. albida* tree at both soil depths (Tab. A.3). The effects of the position from *F. albida* trees on all measured soil properties can be found in Table A3 of the Supplementary material.

3.4. Range (distance) of influence of the trees assessed from geostatistics

In groundnut (plot A, Fig. 6a, 3rd flight), the largest NDVI (groundnut & weeds) values predominated close to *F. albida* trees and beneath. The further from the trees, the lower the NDVI values (tan pixels revealing bare soil). The same observation was made for the other indices (GNDVI, CTVI and MSAVI2).

The directional semi-variograms generated based on distance from *F. albida* tree crowns showed no significant influence of azimuth on their shape. The system was therefore assumed to be isotropic (i.e., the spatial correlation of the data depends only on the distance and not on the azimuth). The best-fitted model obtained for the groundnut NDVI signal was "Ste" (Spherical) with a nugget of zero (i.e., suggests no measurement error), exhibiting a consistent and asymptotic pattern (Fig. 7a). The "Range" parameter, representing the statistical distance over which the *F. albida* tree influences the groundnut NDVI, was found to be 9.8 m (Fig. 7a). Similarly, the "Range" was 9.6 m for CTVI, MSAVI2, and 8.5 m for GNDVI (data not shown). These distances of influence were therefore much less than the distance (25 m) separating the subplots F (far from the tree) from *F. albida* tree.

Due to the plot's heterogeneity, the azimuth significantly influenced the shape of the directional semi-variograms performed for millet (Fig. 7b). The system was therefore assumed to be anisotropic (i.e., the spatial correlation of the data depends on the azimuth). Only the semi-variogram at 90° gave a satisfactory result for the fitted models due to the significant East-West (90°-270°) disparity in millet density and performance observed in Plot B. In fact, we observed higher millet density and better performance in the eastern section of Plot B (at 90°; see Fig. 1B). The best fitted semi-variogram model for that direction, for the millet NDVI signal was also "Ste" (Nugget = 0). The "Range"

Table 1
One-way ANOVA statistics for effect of the distance to the proximal *F. albida* tree on the average of some groundnut (gnd) and weeds (wd) crop traits, as assessed in 18 harvest subplots according to 3 distances to the tree: under crown "U", crown edge "E" and far from the crown "F". N = 6 replicates per distance to tree. For vegetation indices, only the subplots visible by the drone (crown edge "E" and far from the crown "F"; N = 12) have been taken into account. Harvest was on 2019/11/04; Maximum groundnut LAI and height was achieved on 2019/10/10. The values within the parentheses represent the standard deviations. Significance of tests: (.) significant at 0.1; (*) significant at 0.05; (**); significant at 0.01; (***) significant at 0.001.

	Variables	Under crown (U)	Edge crown (E)	Far from crown (F)	Variances homogeneity (Bartlett)	Normality of the residues (Shapiro)	Test	F-value	p-value
Plant variables at harvest (2019/11/04)		a	a	a					
	Pod Dry Mass_harvest (g m^{-2})	80.88 (15.08)	76.19 (22.12)	73.37 (18.75)	0.72	0.36	ANOVA	0.242	0.788
		a	a	a					
	Leaf Dry Mass_harvest (g m^{-2})	20.97 (7.02)	16.68 (6.45)	16.65 (5.07)	0.78	0.63	ANOVA	0.96	0.405
		a	ab	b					
	Stem Dry Mass_harvest (g m^{-2})	43.12 (9.71)	33.84 (13.19)	25.5 (7.9)	0.54	0.84	ANOVA	4.23	0.035 *
		a	a	a					
	Haulm Dry Mass_harvest (g m^{-2})	64.08 (15.24)	50.52 (18.59)	42.15 (12.65)	0.71	0.54	ANOVA	2.99	0.080
		a	a	a					
	Root Dry Mass_harvest (g m^{-2})	9.49 (1.84)	9.52 (2.97)	9.62 (2.44)	0.6	0.99	ANOVA	0.004	0.996
		a	a	a					
	Whole-plant Dry Mass_harvest (g m^{-2})	154.45 (29.36)	136.23 (42.5)	125.14 (33.47)	0.72	0.61	ANOVA	1.04	0.377
		a	a	a					
	Weeds aerial Dry Mass_harvest (g m^{-2})	92.17 (33.65)	78.12 (40.11)	52.01 (23.44)	0.53	0.78	ANOVA	2.27	0.138
		a	a	a					
	Litter Dry Mass (gnd root +wd) _harvest (g m^{-2})	101.66 (32.33)	87.64 (38.25)	61.63 (22.68)	0.55	0.82	ANOVA	2.46	0.120
		a	a	a					
	SLA_gnd_harvest ($m^2_{leaf_gnd}$ $kgDM^{-1}$)	13.86 (1.35)	13.3 (0.6)	13.16 (0.8)	0.21	0.36	ANOVA	0.86	0.443
		a	a	a					
	LAI_gnd_harvest ($m^2_{leaf_gnd}$ m^{-2}_{soil})	0.30 (0.11)	0.22 (0.10)	0.22 (0.06)	0.5	0.5	ANOVA	1.4	0.280
		a	ab	b					
	LAI_harvest gnd + wd ($m^2_{leaf_gnd_wd}$ m^{-2}_{soil})	1.56 (0.42)	1.25 (0.42)	0.91 (0.32)	0.79	0.59	ANOVA	4.16	0.036 *
		a	ab	b					
	Maximum number of leaves per gnd plant (-)	48.18 (13.15)	41.08 (5.18)	34.15 (4.44)	0.04	0.02	Kruskal-Wallis	-	0.030 *
		a	ab	b					
	Maximum gnd height (cm)	39.24 (8.59)	31.83 (5.84)	24.13 (3.98)	0.27	0.29	ANOVA	8.3	0.004 **
Plant variables at maximum (2019/10/10)		a	ab	b					
	Maximum Gnd Leaf Dry Mass (g m^{-2})	103.06 (34.49)	77.56 (29.74)	43.88 (13.36)	0.15	0.32	ANOVA	7.04	0.006 **
		a	ab	b					
	Maximum Gnd Haulm Dry Mass (g m^{-2})	146.18 (41.49)	111.41 (40.83)	69.39 (20.74)	0.78	0.13	ANOVA	6.97	0.007 **
		a	ab	b					
	Maximum Gnd LAI (m^2_{leaf} m^{-2}_{soil})	1.44 (0.53)	1.04 (0.44)	0.57 (0.17)	0.5	0.5	ANOVA	6.61	0.009 **
Vegetation indices		-	a	a					
	NDVI of Gnd & Wd 2019/09/05 (1st flight)	-	0.36 (0.02)	0.37 (0.01)	0.21	0.1	ANOVA	2.04	0.21
			a	a					
	MSAVI2 of Gnd & Wd 2019/09/05 (1st flight)	-	0.28 (0.06)	0.26 (0.05)	0.49	0.89	ANOVA	0.28	0.610
		a	b	c					
	NDVI of Gnd & Wd 2019/10/29 (3rd flight)	0.43 (0.00)	0.35 (0.03)	0.27 (0.03)	0.93	0.90	ANOVA	28.81	< 0.001 ***
		a	b	b					
	MSAVI2 of Gnd & Wd 2019/10/29 (3rd flight)	0.46 (0.02)	0.16 (0.02)	0.13 (0.03)	0.26	0.71	ANOVA	265.40	< 0.001 ***
		a	b	c					
	GNDVI of Gnd & Wd 2019/10/29 (3rd flight)	0.48 (0.02)	0.35 (0.03)	0.27 (0.03)	0.39	0.93	ANOVA	74.30	< 0.001 ***
		a	a	a					
	Gnd NDVI 2019/10/29 (3rd flight)	0.18 (0.05)	0.14 (0.06)	0.11 (0.04)	1.34	0.95	ANOVA	3.2	0.06
		a	a	a					

(*continued on next page*)

Table 1 (*continued*)

	Variables	Under crown (U)	Edge crown (E)	Far from crown (F)	Variances homogeneity (Bartlett)	Normality of the residues (Shapiro)	Test	F-value	p-value
	Gnd MSAVI2 2019/10/29 (3rd flight)	0.08 (0.02)	0.07 (0.03)	0.06 (0.02)	1.66	0.95	ANOVA	1.32	0.26

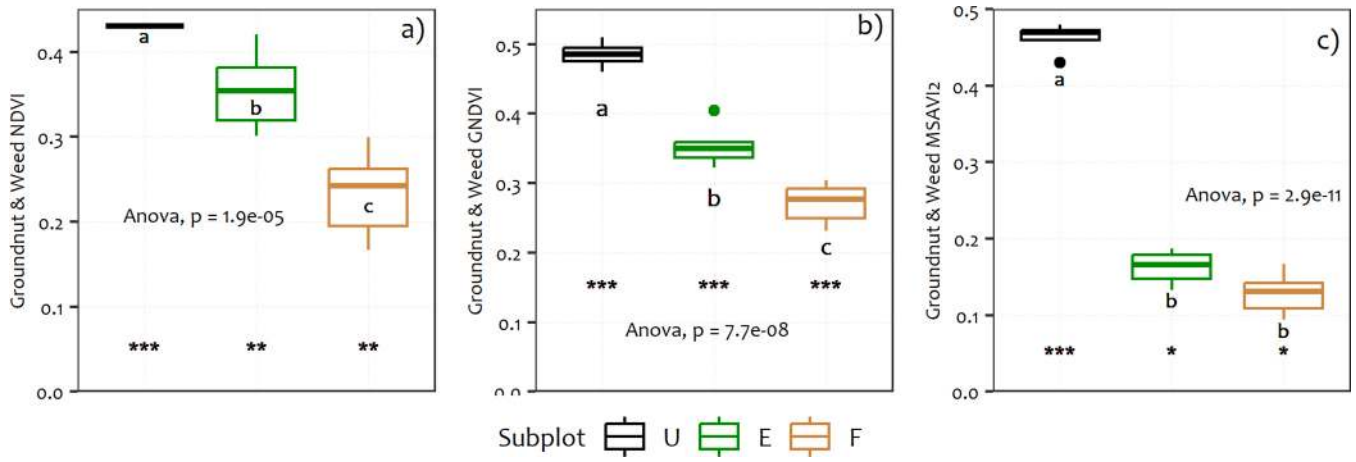


Fig. 5. Effect of the distance to *F. albida on groundnut plot vegetation indices (NDVI, GNDVI and MSAVI2).* ***(a)–(c), vegetation indices for "groundnut + weeds" (measured via camera suspended from a 2.5 m high pole during the third flight, close to harvest on 2019/10/29). (ns) Not significant; (**) significant at 0.05; (**); significant at 0.01; (***) significant at 0.001.***

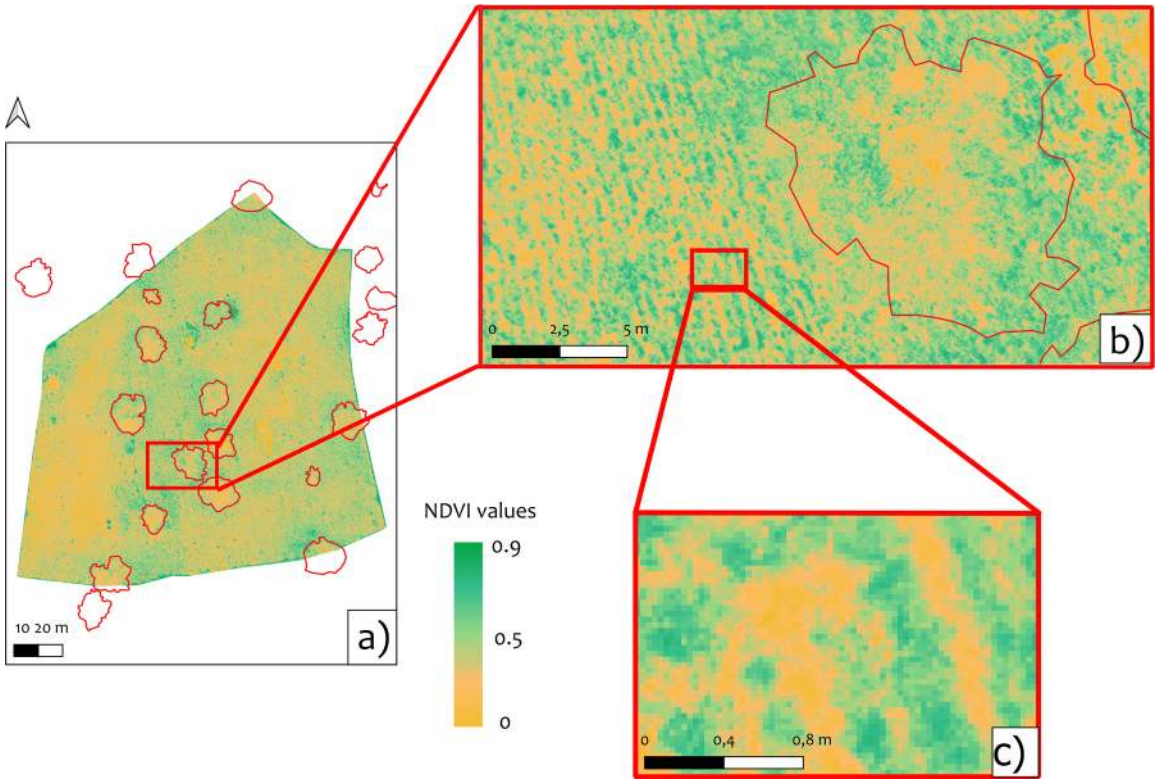


Fig. 6. NDVI of "groundnut + weed" sensed by UAV above the agroforestry plot A (see Fig. 1A), five days before the groundnut harvest (2019/10/29, 3rd flight). The greener the color, the higher the NDVI. **a/ NDVI of "groundnut + weed" image of the whole-plot, with tree crows in red; b/ zoom on one tree, showing greener pixels (more groundnut + weed foliage) in the vicinity of the tree (which is defoliated during the crop season); c/ zoom showing the groundnut rows in green and inter-rows in tan at maximum resolution (one pixel = 5.4 cm^2).**

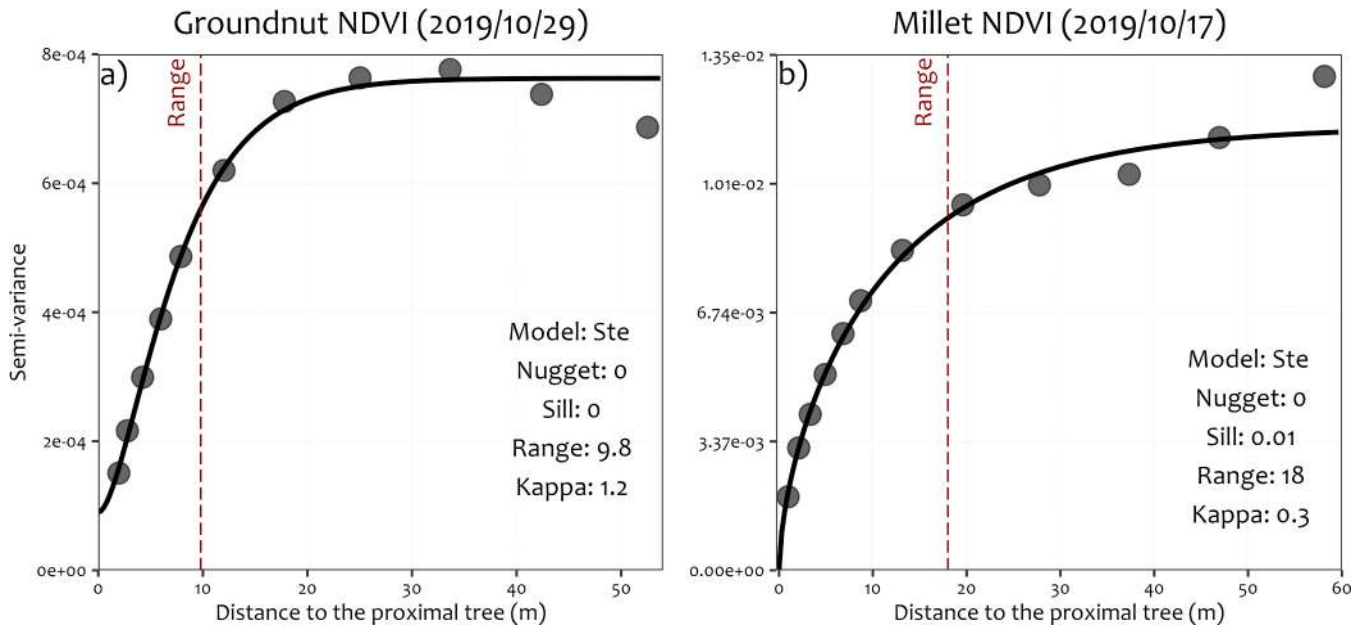


Fig. 7. a/ Geostatistics to estimate the distance of influence of the *F. albida* tree on crops (groundnut or millet) NDVI close to harvest (third flight). Semi-variograms between NDVI of all grid cells in the whole-plot cultivated with crops and the distance to the proximal Faidherbia tree crown. The "Range" parameter or distance of influence was computed with 'Ste' model (vertical red dotted line). The semi-variograms obtained by other models were very similar to 'Ste'. a/ Groundnut, the "Range" or distance of influence is 9.8 m; b/ Millet: the "Range" is 18 m.

parameter was 18 m (Fig. 7b), i.e. twice as long as for groundnut.

3.5. Upscaling yield, from sub to whole-plot

3.5.1. Whole plot yield estimated from UAV and geostatistics

In Section 2.3.3, we estimated the sole groundnut vegetation indices signals (referred to as groundnut-only signal below) from the overall

Table 2
Statistical correlations between some groundnut or millet traits and vegetation indices (NDVI, GNDVI and MSAVI2) and between the corrected groundnut LAI and the pod yield. Significance of tests: (.) significant at 0.1; (*) significant at 0.05; (**); significant at 0.01; (***) significant at 0.001. 1st flight, 2nd flight, and 3rd flight were carried out on 2019/09/05, 2019/10/17, and 2019/10/29 respectively.

	Fig. 8	Y Variable	X Variable	Z Variable	W Variable	Equation	Normality of the residues (Shapiro)	r^2	RMSE	p-value
Groundnut	a	Groundnut pod yield (g m^{-2})	Groundnut MSAVI2 «3rd flight »	Groundnut NDVI «3rd flight »	-	Y = 1206.59X - 330.19Z + 40.12	0.59	0.73	9.8	0.003 **
	b	Groundnut haulm yield (g m^{-2})	Groundnut MSAVI2 «3rd flight »	-	-	Y = 541.22X + 12.24	0.98	0.85	5.81	< 0.001 ***
	c	Groundnut total dry mass (g m^{-2})	Groundnut MSAVI2 «3rd flight »	-	-	Y = 1212.49X + 54.30	0.4	0.78	16.56	< 0.001 ***
	d	Groundnut LAI (m^2_{lea} m^{-2}_{soil})	Groundnut MSAVI2 «3rd flight »	MSAVI2 «1st flight »	GNDVI «3rd flight »	Y = 3.06X - 0.38Z - 0.21 W + 0.20	0.19	0.98	0.01	< 0.001 ***
		Litter biomass (g m^{-2})	MSAVI2 «3rd flight »	NDVI «1st flight »	-	Y = 803.7X + 649.4Z - 279.2	0.59	0.62	19.47	0.01 *
		Groundnut pod yield (g m^{-2})	Groundnut LAI Cor ($m^2_{leaf}m^{-2}_{soil}$)	-	-	Y = 17.43X + 59.06	0.16	0.26	3.74	0.029 *
Millet	-	Millet grains yield (g m^{-2})	NDVI	MSAVI2	-	Y = 1467.89X + 2069.85Z - 16.21	0.36	0.74	20.48	0.002 **
	-	Millet leaves biomass (g m^{-2})	NDVI	MSAVI2	-	Y = 594.46X - 911.01Z + 26.25	0.54	0.61	13.3	0.01 *
	-	Millet stems biomass (g m^{-2})	GNDVI	MSAVI	-	Y = 1577.4X - 1159.3Z - 349	0.26	0.72	28.34	0.003 **
	-	Millet total biomass (g m^{-2})	NDVI	MSAVI2	-	Y = 4670.5X - 6775Z - 47.2	0.06	0.66	85.87	0.008 **
	-	Millet LAI (m^2_{lea} m^{-2}_{soil})	NDVI	MSAVI2	-	Y = 5.59X - 8.24Z - 0.17	0.65	0.50	0.15	0.05 *
	-	Litter biomass (g m^{-2})	GNDVI	MSAVI	-	Y = 2679.7X - 2065.6Z - 557.1	0.42	0.70	51.78	0.004 **

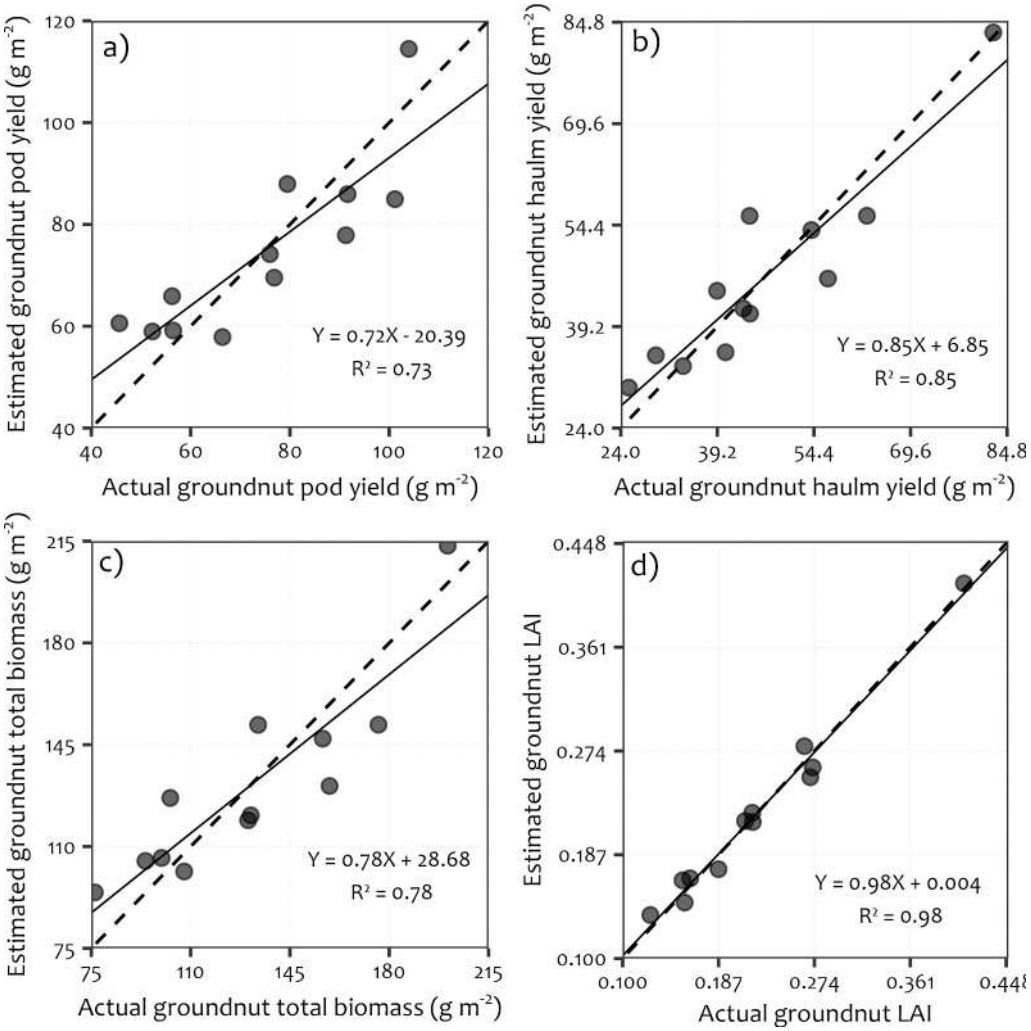


Fig. 8. a–d/ Scatter plots comparing estimated groundnut traits, derived from the correlation (referenced in Table 2) between vegetation indices and groundnut traits in the subplots visible by the drone (E and F only; N = 12), with measured groundnut traits collected from the same subplots. Each dot represents one subplot from experiment number 2 (Fig. 1A). Thick black lines represent the respective linear regressions, while dashed black lines indicate the 1:1 lines.

vegetation indices (which include signals from both groundnut and weeds, referred to as groundnut + weeds signal below). Table 2 presents the statistical correlations between various groundnut traits and vegetation indices (groundnut-only signal and groundnut + weeds signal for NDVI, GNDVI, and MSAVI2). Fig. 8 presents scatter plots comparing the estimated groundnut traits derived from the correlations listed in Table 2 with the actual groundnut traits measured from the same subplots.

The results reveal significant positive correlations between groundnut traits and vegetation indices (Table 2). These correlations were established by analyzing consecutive images of vegetation indices through multiple linear regressions (stepwise regression). Specifically, pod yield was strongly correlated with MSAVI2 (groundnut-only signal) and NDVI (groundnut-only signal) of the 3rd flight (Table 2 & Fig. 8a; $r^2 = 0.73$; RMSE = 9.8 g m^{-2}). Similarly, both groundnut haulm yield and total groundnut biomass showed strong correlations with MSAVI2 (groundnut–only signal) of the 3rd flight (haulm yield vs MSAVI2: Table 2 & Fig. 8b; $r^2 = 0.85$; RMSE = 5.81 g m^{-2} and total groundnut biomass vs MSAVI2: Table 2 & Fig. 8c; $r^2 = 0.78$; RMSE = 16.56 g m^{-2}). Furthermore, a strong positive correlation was found between the LAI and the MSAVI2 signal from the 1st flight, as well as the GNDVI (groundnut + weeds signal) and MSAVI2 (groundnut-only signal) from the 3rd flight (Table 2 & Fig. 8d; $r^2 = 0.98$; RMSE = 0.01 $m^2_{leaf}\, m^{-2}_{soil}$). The litter biomass also exhibited strong correlations with MSAVI2 (groundnut + weeds signal) of the 3rd flight and NDVI of the 1st flight (Table 2; $r^2 = 0.62$; RMSE = 19.47 g m^{-2}).

We also looked for correlations between groundnut traits by simple linear regression. Thus, a significant but weak positive correlation was found between the pod yield and the groundnut maximum LAI (Table 2; $r^2 = 0.26$; RMSE = 3.74 g m^{-2}). In Table A4 of the Supplementary material we also show results for correlations between groundnut traits and each vegetation index by simple linear regression. Overall, combining sequential images of vegetation indices in multiple linear regressions significantly improves predictions (Tab. A4).

Using the equations derived from the correlations between pod yield and vegetation indices, as well as between haulm yield and vegetation indices (Table 2), we could finally estimate the pod and haulm yields for the whole-plot. On the yield maps (Fig. 9) produced from these relationships, we can see more haulm yield and litter biomass close to *F. albida* trees (Fig. 9b and c). The estimated pod yield for the whole plot was 0.81 h^{-1} (Table 3), the estimated haulm yield was 0.52 h^{-1} (Tab. A5).

In Table 2, we also looked for correlations between millet traits and vegetation indices (NDVI, GNDVI, MSAVI and MSAVI2) of the drone flight carried out a couple of days before millet harvest (2019/10/17). We found that the multiple linear regression model explains 74 % of the variability in millet yield (RMSE=20.48 g m^{-2}) when using the MSAVI2 and NDVI signals for millet and weeds (Table 2). Both millet total

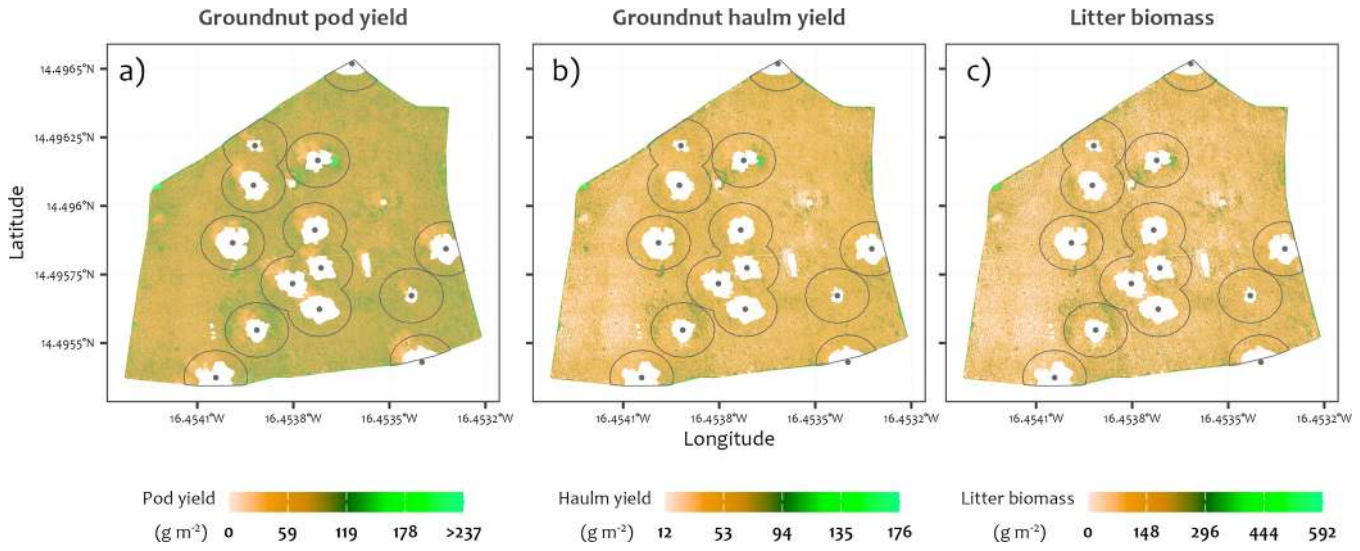


Fig. 9. Maps of groundnut productivity (biomass of yield, haulm and litter) at the whole-plot scale (ca. 1 ha), obtained using the correlations from Table 2 between subplot harvest and vegetation indices. Gaps are for the position of the *F. albida trees. Grey dots represent the centroids of F. albida canopies, while areas with grey borders indicate the zones of influence of F. albida on groundnut, as computed through geostatistics.*

biomass and LAI were positively correlated with NDVI and MSAVI2 (Table 2; millet total biomass vs NDVI+MSAVI2: $r^2 = 0.66$; RMSE = 85.87 g m^{-2} and millet LAI vs NDVI+MSAVI2: $r^2 = 0.50$; RMSE = 0.15 m^2_{leaf} m^{-2}_{soil}). A positive and significant correlation was found between millet stem biomass, GNDVI and MSAVI signals (Table 2; $r^2 = 0.72$; RMSE = 28.34 g m^{-2}). The litters biomass was also correlated with GNDVI and MSAVI2 signals (Table2; $r^2 = 0.70$; RMSE = 51.78 g m^{-2}).

3.5.2. *Actual groundnut whole-plot yields of pods and haulms*

At harvest, small heaps of groundnuts were put together by the farmers. Of the 988 heaps made for the whole-plot A, 104 heaps were weighed in the field. On average, each heap weighed 2.61 ± 0.69 SD kg. From the ratio of conversion from fresh heap (leaf + stem + pod) to dry pod obtained in the subplots (0.37 ± 0.05 SD), we computed a harvest of 954.33 kg_{pod} at which the 22.28 kg_{pod} obtained in the subplots were added, making a total of 976.61 kg_{pod} for the whole-plot (Table 3). On an area of 11,080 m^2, we thus had a yield of 0.88 t_{pod} ha^{-1}. With the same method, the total haulm biomass for the whole-plot was estimated at 645.29 kg_{haulm}. The haulm yield was 0.58 t_{haulm} ha^{-1} (Tab. A5).

3.6. *Groundnut LERcp*

Table 3 and A5 present the LERcp for pod and haulm yields, respectively. For pod yield, LERcp was calculated as 1.02, which was the same whether the whole-plot yield or the yield from the area beneath the Range was used (Table 3). In contrast, haulm yield showed a LERcp of 1.05 when based on the whole-plot yield, whereas the LERcp increased to 1.11 when the yield from the Range area was considered (Table A5).

4. Discussion

4.1. *Dynamics of groundnut growth and leaf shedding*

Groundnut growth is largely influenced by environmental and seasonal conditions. However, it generally follows four phases, namely: (i) the lag phase at the beginning of growth; (ii) the exponential weight increase, from the vegetative to the flowering stage; (iii) linear growth until maximum, between the end of the vegetative stage and the beginning of pod filling; and (iv) the maturation during the late pod filling phase (Singh, 2003). The first three phases were observed in the first 9 weeks after sowing. In the last three weeks before harvest, during the pod filling stage, a drop of about 52 % in leaf biomass was observed. Assuming that groundnut leaves become less effective with age (Singh, 2003), we could attribute this drop to the fact that in this period the plant prioritizes and invests much more in pod formation and filling, retranslocating the reserves from the leaves to the pods, which causes senescence and then leaf drop. Henning et al. (1979) reported a reduction in the photosynthetic capacity of the leaves in this period due to their contributions to pod formation. We also observed early leaf spots on the groundnut plants before the leaf drop. According to Olatinwo and Hoogenboom (2014) this is generally caused by the 'black Sigatoka' (*Cercospora arachidicola* S. Hori), a significant fungal pathogen responsible for a severe foliar disease in groundnuts, which can lead to the complete defoliation of susceptible cultivars. This foliar disease is rampant in Senegal with a level of maximum severity towards the maturity of the pods (Zongo et al., 2019).

In the agro-silvo-pastoral systems of the groundnut basin, groundnut haulm is one of the fodder resources used to feed livestock during the dry season. This drop in leaf could therefore contribute to a reduction in the amount of haulm that farmers should have had after harvest. Nevertheless, leaves that will not be exported, could contribute to the storage of carbon in the soil, and therefore the enrichment of the soil through their degradation if they are not carried away from the plot by wind. There would therefore be an important trade-off, agronomically speaking, between harvesting the haulms a little earlier to maximize the forage resource, but this to the detriment of pod filling, or alternatively prioritizing pod filling and restitution to the soil via the supply of dead leaves and other crop residues to the soil after harvest. A second trade-off is between exporting the haulms or incorporating them into the soil to promote the next crop or even free grazing in the field to ingest the haulms and return them to the field via their faeces. However, if the leaf drop is linked to the severity of the black Sigatoka, this reasoning above should be mitigated. Let's also point out that dropping leaves would also recharge the soil with the fungus spore.

4.2. *Groundnut performance relative to distance from F. albida trees*

Numerous authors reported a positive impact of *F. albida* on crops like maize (Dilla et al., 2018; FAO, 2016), millet (Leroux et al., 2020; Roupsard et al., 2020) and several other cereals (Hadgu et al., 2009; Sida et al., 2018), through studies in Central and West Africa. In the literature, this positive impact of *F. albida* on agroforestry crops is frequently ascribed to a set of biological processes (Kho et al., 2001), changes in physical and chemical conditions of the soil (Poschen, 1986) and

Table 3
Scaling-up of groundnut yields (pod) and crop Land Equivalent Ratio (LERcp) from subplots to the whole-plot scale and comparison (error) between measurements (in subplots and at the whole-plot scale) and estimations through UAVs NDVI & MSAVI2 product.

	Method	Variable of interest	Value	Unit
Area	QGIS	Whole plot area	11,144	m^2
	QGIS	Shelter area	62	m^2
	QGIS	Trunk basal area	2.4	m^2
	QGIS	Whole plot effective area	11,080	m^2
	Measured	Subplots area (Experiment 2)	290.58	m^2
	QGIS	*F. albida* canopy projected area	982.50	m^2
	QGIS	*F albida* canopy cover	8.8	%
	QGIS	Area (dist > Range)	8182.5	m^2
	QGIS	Area (Crown < dist < Range)	2088.9	m^2
Pod	Measured	Subplots harvest (Experiment 2)	22.28	kgDM pod
Harvest	Measured	Number of the whole-plot heap harvest (without subplots)	998	# heap
	Measured	Weight of the whole-plot heap harvest (without subplots)	2604.9	kgDM heap
	Measured	Rate of conversion heap-to-pod	0.37	/
	Measured	Whole-plot pod harvest (without subplots)	954.33	kgDM pod
	Measured	Whole-plot harvest	976.61	kgDM pod
	UAV-MSAVI2&NDVI (Estimated)	Estimated Whole-plot harvest	902.83	kgDM pod
Pod	Measured	Groundnut yield below Faidherbia crown (U)	0.81	tDM pod ha^{-1}
Yield	Measured	Groundnut yield at the edge of Faidherbia crown (E)	0.76	tDM pod ha^{-1}
	Measured	Groundnut yield as sole crop (F)	0.73	tDM pod ha^{-1}
	Measured	Whole-Plot Yield	0.88	tDM pod ha^{-1}
	UAV-MSAVI2&NDVI (Estimated)	Estimated Groundnut yield sole crop (dist > Range)	0.80	tDM pod ha^{-1}
	UAV-MSAVI2&NDVI (Estimated)	Estimated Groundnut yield agroforestry (Crown < dist < Range)	0.81	tDM pod ha^{-1}
	UAV-MSAVI2&NDVI (Estimated)	Estimated Groundnut yield agroforestry (dist < Crown)	0.82	tDM pod ha^{-1}
	UAV-MSAVI2&NDVI (Estimated)	Estimated Whole-plot Yield	0.81	tDM pod ha^{-1}
	Error	Yield Error	8.17	%
LER for	UAV-MSAVI2&NDVI (Estimated)	LERcp with Yi = actual whole plot yield	1.02	/
pod	UAV-MSAVI2&NDVI (Estimated)	LERcp with Yi = whole plot yield for Crown < dist < Range	1.02	/

changes in environmental conditions caused by *F. albida* in the system (Barnes and Fagg, 2003). In our study, groundnut pod yield was not significantly affected by distance to *F. albida* (Fig. 4a). This result is new as compared to previous studies where authors often reported a depressive effect of *F. albida* on groundnut pod yield. In fact, a similar study in Senegal reported a significant depressive effect (loss of 24 % of pod yield) in the first three meters around the trunk of *F. albida* (Louppe et al., 1996). These authors hypothesized that it was due to excess nitrogen in the soil or shade at the time of flowering, caused by the woody parts then since *F. albida* is defoliated during the wet season. In northern Cameroon, another study demonstrated a decrease in groundnut pod yields by 34 % when grown under young plants of *F. albida* (Harmand and Njiti, 1992). In the latter study, the negative impact of *F. albida* was linked to the high planting density, which obstructed plowing operations and reduced the available arable area. Additionally, the small crown size and low foliar biomass production of the young *F. albida* plants (5-years old) resulted in no discernable positive effects on soil fertility or crop yields. Overall, this confirms that unlike cereals, groundnuts do not perform better in terms of pod yield when associated with *F. albida.* The absence of a negative effect of *F. albida* on groundnut pod yield observed in this study was rather unexpected, especially given the higher incidence of the black Sigatoka infestation under the trees. The haulm yield estimated before leaf fall was clearly and significantly higher (multiplied by 1.5) closer to *F. albida* (Table 1). But, probably because of the higher incidence of black Sigatoka under the trees at senescence phase, groundnut haulm yield at harvest was no more significantly affected by distance to *F. albida* at the harvest time ($p = 0.08$) (Fig. 4b and Table 1). Louppe et al. (1996) also reported a significant improvement in the groundnut haulm yield by trees of *F. albida* in the groundnut basin of Senegal (a gain of about 23 % of haulm yield under tree, compared to the control outside *F. albida* influence). This could be attributed to the availability of water and nitrogen under the tree crown during the vegetative phase of the crop. We have not seen any effect on SLA, although it is often reported in the literature to decrease in shaded conditions (Matos et al., 2009).

F. albida significantly affected the vegetation indices of "groundnut + weeds" tested during the last UAV flight (2019/10/29) (Fig. 5). However, the large values of the indices obtained near the trees could be due, on one hand, to the fact that fresh litter continues to contribute to the vegetation indices (Van Leeuwen and Huete, 1996), and on the other hand, to the presence of weeds. The vegetation indices estimated solely for groundnut were unaffected by proximity to *F. albida* (Table 1), likely due to the decline in groundnut leaf cover prior to the final drone flight.

4.3. Soil nutrient status according to distance from F. albida trees

For this study, no fertilizer was applied to the plots. The greater nitrogen (%N), carbon (%C) and organic carbon contents found under *F. albida* crowns as compared to subplots that are far from the tree corroborate the results of many studies (Dilla et al., 2018; Umar et al., 2013). However, we found no significant impact of *F. albida* on the soil properties such as: available P, pH (H_2O and KCl), C/N and exchangeable cations (Ca, Mg, Na and K), although several studies have highlighted an increase in available P (Kho et al., 2001; Umar et al., 2013), pH and exchangeable cations (Ca (100 %), Mg (48 %), K and Na (30–40 %)) under *F. albida* trees compared to open fields located far away from trees (CTFT, 1988). Charreau and Vidal (1965) found that the rate of nitrogen under the tree doubles, unlike carbon, which implies that the C/N ratio decreases the closer to the tree and there is a rapid mineralization of organic matter under the tree. Authors often attributed this soil fertility under *F. albida* to the quantity of leaves and pods which fall under the tree crowns as well as the bark and the wood which are detached each season providing important minerals to the soil (Jung, 1970). The input of these nutrients (e.g., organic carbon) is also favored by the phenological inversion of *F. albida*. Indeed, this input is made at the end of the dry season, at the peak of agricultural activity, and is promptly integrated into the soil when the microbiological activity is at its highest (CTFT, 1988). The influence of livestock through feaces droppings is also mentioned to explain this fertility but it remains marginal according to Charreau and Vidal (1965) who showed at Bambey (Senegal) strong enrichments under trees, independently of the livestock.

4.4. Improving crop traits estimation with UAV; using several MS images along crops cycle

Roupsard et al. (2020) used one single UAV MS image to explain 47 % of millet variability using millet+weeds MSAVI2 in the same plot A than for our study, cultivated with millet during the year 2018. Here, we aimed to improve their correlation by using multiple MS images throughout the crop cycle. In fact, in agro-silvo-pastoral systems, even at plot scale, spatial patterns may emerge during the season, especially due to the varying impact of the tree on the crop all along the cropping season, the influence of weeds and of crop leaf senescence, for instance. To take advantage of several UAV MS images along the crop cycle was expected to properly capture these temporal aspects in the observed spatial patterns, and consequently to strengthen correlations between crop traits and vegetation indices.

Indeed, for millet in 2019, the multiple linear regression model explains 74 % of the variability in millet yield (RMSE = 20.48 g m^{-2}) using millet and weeds MSAVI2 and NDVI signals, which is a large improvement, as compared to 47 % obtained by Roupsard et al. (2020). Considering groundnut now, where no equivalent is available in the literature, we obtained positive correlations between groundnut pod and haulm yields and vegetation indices. Whatever the crop (millet or groundnut), combining the sequential images of vegetation indices into multiple linear regressions significantly improves the relationships. Leroux et al. (2020) proposed a remote-sensing based model in the groundnut basin of Senegal that explained 48–70 % of millet yield variability, depending on the vegetation proxy used. They found that incorporating proxies of parkland structure enhanced the model's accuracy, although capturing yield variability in small plots (e.g., 1 ha) using satellite images can be challenging. UAV-based models are more suitable to fully capture intra-plot variability, as also reported by Diene et al. (2024) for millet. We estimated groundnut pod yields of the whole-plot with only 8 % error with comparison to the whole-plot harvest reference, which is also a large improvement as compared to Roupsard et al., (2020) (20 % error). In spite of potential errors inherent to the reference method itself, this good match between measured and estimated yield is probably due to the strength of our correlations between groundnut yields (pod and haulm) and VIs (NDVI and MSAVI2).

4.5. Groundnut LERcp estimation for pod and haulm yields

The groundnut LERcp of 1.02 for pod yield and 1.05 for haulm yield sounds rather marginal. Using a more classical way to assess the *F. albida* effect on groundnut, Louppe et al. (1996) found an overall depressive effect of *F. albida* on groundnut pod yield up to at least 10 m from the tree's trunk and predicted a pod yield loss between 2.4 % and 2.8 % in a parkland of 5 trees ha^{-1}. For millet grain yield, Roupsard et al. (2020) found on the same plot a year before, a LERcp of 1.10. Apart from the tree and crop species, the annual variability, the parkland configuration, especially the tree density, affects the ability of the system to outperform monoculture systems in terms of crop yield (Leroux et al., 2020). Several parkland configurations (e.g., different tree densities) could be tested in association with different crops through modeling to determine which parkland configuration gives the best outputs in terms of benefits such as LERcp (or crop yields improvement).

4.6. Current limitations of the method and options for improvements

Roupsard et al. (2020) stated that the 'Range' is valid only for the crop spectral index measured by the UAV and traits strongly correlated with it. The better the correlation between the spectral index and the crop trait, the more accurately the Range represents the limit of influence. Thus, the relationship between the spectral index and crop trait is key in determining the distance of influence. Here, the relationship between crop traits and NDVI are linear, simplifying the estimation of the distance of tree's influence. However, if the relationship were non-linear or saturating, estimating the distance of tree's influence would become more complex.

This work build on the study by Roupsard et al. (2020) on millet by applying their approach to groundnut crops, introducing methodological improvements (e.g., use of multiple MS images throughout the crop cycle), and validating the findings for millet one year later. We combined the sequential images of vegetation indices into multiple linear regressions to strengthen correlations between crops traits and vegetation indices. Further improvements of this approach could be: (i) UAV flights at key times of the groundnut and millet phenological cycle and (ii) weeds removal before the last UAV flight to only have the crop VIs signals on the last UAV image. Incorporating machine learning models can also offer the potential to propose a unique model of yield prediction for crops under agroforestry (Diene et al., 2024).

Additionally, we acknowledge the absence of Black Sigatoka assessment as a potential confounding factor. Since we did not quantify the extent of leaf spotting within our subplots during the field campaign, we lacked the necessary data to incorporate this variable into our statistical analysis. Future studies could address this limitation by systematically evaluating disease severity (if present) to better isolate its potential effects. Although maximum leaf biomass was computed to assess the influence of tree proximity on leaf development, these estimates were not used in the remote sensing calibration for yield prediction. We recognize that uncertainties are associated with these values, as destructive sampling could not be conducted at that stage due to the need to allow the crop to reach full maturity. This constraint limited our ability to directly validate the maximum biomass values but did not affect the core remote sensing analysis. A further limitation might relate to tree density. In our study site, trees were sparsely distributed, which allowed us to position subplots sufficiently far from tree influence, enabling the calculation of LERcp. However, in denser agroforestry systems, where trees may be spaced 10 m apart or less, it would be difficult, if not impossible, to find areas without tree influence. This constraint could limit the applicability of our method in such settings.

4.7. The distance of tree influence on crops can serve as a reliable proxy for its impact on crop performance

The assessment of agroforestry tree impacts on crops and on LER are of paramount importance for supporting and restoring agroforestry practices, however, they remained challenging for long, especially due to the heterogeneity introduced by trees in agroforestry parklands and the cost of the different methodologies used by researchers to evaluate it. For example, most past studies used complex, time-consuming and costly field experiments (Louppe et al., 1996; Tomlinson et al., 1998). Taking into account the heterogeneity induced by trees and to alleviate the work of experimentation in the field, Bayala et al. (2015) suggested to combine yield mapping and geostatistics to assess the impact of trees on crop performance.

The flexibility and advantages of the use of UAVs (e.g., low price and high-resolution images) offers the opportunity to develop this approach. In a previous study, Roupsard et al. (2020) reported that *F. albida* affects millet yield up to 17 m. In this study, we found a Range of 9.8 m (Fig. 7a), i.e. twice as low as for millet, indicating that the groundnut NDVI was influenced by trees only up to that specific distance. Indeed, we also confirmed the Range results of Roupsard et al. (2020) on millet, on the same cropping system (same soil, same farmer, same practices, relatively same tree density) but on another plot and for a subsequent year. This confirmation suggests that the method seems to be robust enough to develop other spatial and temporal comparisons.

Even if we do acknowledge the influence of interannual and inter-plot variability in the estimation of the Range (no data for confirmation yet), we report here both a higher Range and a higher effect on yield for the cereal (not N-fixing) than for the groundnut (N-fixing). With a new UAV and geostatistics method, we confirm previous studies reporting that overall, the effect of *F. albida* on groundnut is lower (can

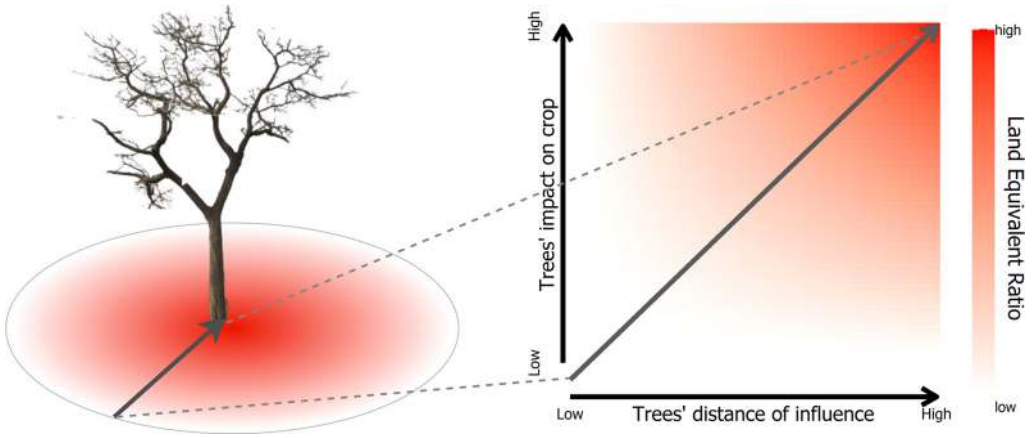


Fig. 10. Illustration of the relationships between the impact of *F. albida on crops, the distance of tree influence on crops, and the crop Land Equivalent Ratio (LERcp).*

be negative) than on millet (usually positive).

The new finding here is that a lower effect on the crop is accompanied by a shorter distance of influence and a lower LERcp (Fig. 10). This simple observation suggests an opportunity in estimating the importance of the tree effect through a proxy, namely the 'Range', or distance of influence. We stress that the distance of influence is easy to measure and statistically sound (with a very high number of pixel replicates in a single plot), whereas the importance of the tree effect was so tedious to measure and to replicate in the past. Therefore, the distance of influence (the geostatistical 'Range'), is worth testing in various conditions and could be promoted as a proxy of the strength of the effect and of the LER, averaged at the scale of a whole plot.

If confirmed, such a proxy could even be useful at the intra-plot scale, for any given tree inside the plot. For a single *F. albida* tree taken randomly on a plot, the distance of influence might depend also on the importance of the tree crown or of whether or not the tree has been pruned for instance. In this case, this approach could be applied to every single tree and the standard deviation of the Range, more than its average, could be useful too. In a study carried out in Ethiopia, Dilla et al. (2018) found that maize yield was higher under pruned *F. albida* compared to yield under unpruned trees. They partially attributed this result to reduced PAR (Photosynthetically active radiation) available to crops under unpruned trees. In such a situation, the distance of influence might be greater for pruned trees. There might be a relationship between pruning, the distance of influence and the importance of the tree effect on the crop. However, we appeal for more experiments to confirm this assumption for any agroforestry situation.

5. Conclusions

In this study, we demonstrated that *F. albida* influences groundnut crops but over a shorter distance compared to millet, approximately half the distance, with an estimated distance of influence of 9.8 m for groundnut and 18 m for millet. Notably, the LERcp for groundnut was marginal, 1.02 for pod yield and 1.05 for haulm yield. This reduced positive effect observed on groundnut may be partially explained by the early onset of leaf spot disease, which likely limited the crop's ability to benefit fully from the presence of *F. albida*. However, these results highlight that *F. albida's* influence is crop-dependent, reinforcing the need for species- and crop-specific assessments in agroforestry systems. We saw that *F. albida* has a less substantial impact on groundnut, both in terms of the distance of influence and its effect on groundnut yield, which is reflected in a lower LERcp for groundnut yield. More broadly, we argue that the distance of influence, the "Range", assessed through UAV imagery and geostatistics, can serve as a powerful and efficient proxy to easily assess and rank the influence of agroforestry trees on various crops and estimate the LERcp at the plot scale or even for individual trees, offering a valuable tool for agroforestry system management.

CRediT authorship contribution statement

Louise Leroux: Writing – review & editing, Methodology. **Guerric le Maire:** Writing – review & editing. **Adama Ndour:** Writing – review & editing. **Sekouna Diatta:** Writing – review & editing. **Mame Sokhna Sarr:** Writing – review & editing. **Josiane Seghieri:** Writing – review & editing, Project administration, Funding acquisition. **Alain Audebert:** Writing – review & editing, Methodology, Investigation. **Sanogo Diaminatou:** Writing – review & editing. **Yélognissè Agbohessou:** Writing – review & editing, Writing – original draft, Visualization, Validation, Methodology, Investigation, Formal analysis, Data curation, Conceptualization. **Sidy Sow:** Writing – review & editing, Investigation. **Olivier Roupsard:** Writing – review & editing, Writing – original draft, Visualization, Validation, Supervision, Methodology, Investigation, Conceptualization. **Cathy Clermont-Dauphin:** Writing – review & editing. **Simon Taugourdeau:** Writing – review & editing. **Caroline Pierre:** Writing – review & editing, Project administration, Funding acquisition. **Daniel Fonceka:** Writing – review & editing. **Christophe Jourdan:** Writing – review & editing, Investigation. **Rémi Vezy:** Writing – review & editing.

Declaration of Competing interest

The authors declare that they have no known competing financial interests or personal relationships that could have appeared to influence the work reported in this paper.

Acknowledgments

This research was funded primarily by EU-Leap-Agri RAMSES II and EC2CO ENCAS Projects. The projects EU-DESIRA CASSECS (OOD/2019/410-169), EU-H2020 SUSTAINSAHEL (Grant no. 861974) and EU-Horizon Europe GALILEO (Grant no. 101181623) and ANR-PEPR FairCarbonN/PC3-RIFT also supported this research on the longer term. The authors would like to thank the "Faidherbia-Flux "platform (https://lped.info/wikiObsSN/?Faidherbia-Flux) and the "Laboratoire des Moyens Analytiques" (UAR IMAGO LAMA certified ISO9001:2015) at IRD ("Institut de Recherche pour le Développement") for soil analyses in Dakar (http://www.imago.ird.fr/moyens-analytiques/dakar), Ibou Diouf and Robert Diatte for their help during field campaigns.

Appendix A. Supporting information

Supplementary data associated with this article can be found in the

online version at doi:10.1016/j.agee.2025.109918.

Data availability

Data will be made available on request.

References

Barnes, R.D., Fagg, C.W., 2003. Faidherbia albida: Monograph and Annotated Bibliography. Tropical Forestry Papers. Oxford.

Bayala, J., Sanou, J., Teklehaimanot, Z., Ouedraogo, S.J., Kalinganire, A., Coe, R., Van Noordwijk, M., 2015. Advances in knowledge of processes in soil–tree–crop interactions in parkland systems in the West African Sahel: a review. Agric. Ecosyst. Environ. 205, 25–35.

Bivand, R.S., Pebesma, Edzer, J., Gomez-Rubio, V., Pebesma, Edzer Jan, 2008. Applied Spatial Data Analysis with R. Springer.

Charreau, C., Vidal, P., 1965. Influence de l'Acacia albida del. Sur le sol, nutrition minerale et rendements des mils pennisetum au Senegal. Agron. Trop. 600, 625.

Clermont-Dauphin, C., N'dienor, M., Leroux, L., Ba, Halimatou, S., Bongers, F., Jourdan, C., Roupsard, O., Do, F.C., Cournac, L., Seghieri, J., 2023. Faidherbia albida trees form a natural buffer against millet water stress in agroforestry parklands in Senegal. Biotechnol. Agron. Soc. Environ. 182–195. https://doi.org/10.25518/1780-4507.20477.

Colomina, I., Molina, P., 2014. Unmanned aerial systems for photogrammetry and remote sensing: a review. ISPRS J. Photogramm. Remote Sens. 92, 79–97.

CTFT, 1988. Faidherbia albida (Del.) A. Chev. (Synonyme: Acacia albida Del.): monographie. CIRAD-CTFT, Nogent-sur-Marne, France.

Delaunay, V., 2017. La situation démographique dans l'Observatoire de Niakhar: 1963–2014, 90.

Diack, I., Diene, S.M., Louise, L., Aziz, D.A., Benjamin, H., Olivier, R., Philippe, L., Alain, A., Idrissa, S., Moussa, D., 2024. Combining UAV and Sentinel-2 imagery for estimating millet FCover in a heterogeneous agricultural landscape of Senegal. IEEE J. Sel. Top. Appl. Earth Obs. Remote Sens. 17, 7305–7322. https://doi.org/10.1109/JSTARS.2024.3373508.

Diene, S.M., Diack, I., Audebert, A., Roupsard, O., Leroux, L., Diouf, A.A., Mbaye, M., Fernandez, R., Diallo, M., Sarr, I., 2024. Improving pearl millet yield estimation from UAV imagery in the semiarid agroforestry system of Senegal through textural indices and reflectance normalization. IEEE Access 11. https://doi.org/10.1109/ACCESS.2024.3460107.

Dilla, A.M., Smethurst, P.J., Barry, K., Parsons, D., Denboba, M.A., 2018. Tree pruning, zone and fertiliser interactions determine maize productivity in the Faidherbia albida (Delile) A. Chev parkland agroforestry system of Ethiopia. Agrofor. Syst. https://doi.org/10.1007/s10457-018-0304-9.

Elagib, N.A., Al-Saidi, M., 2020. Balancing the benefits from the water–energy–land–food nexus through agroforestry in the Sahel. Sci. Total Environ., 140509

FAO, 2016. Save and Grow in Practice: Maize, Rice, Wheat: A Guide to Sustainable Cereal Production.

FAO, IFAD, UNICEF, WFP, WHO, 2024. The State of Food Security and Nutrition in the World 2024. FAO; IFAD; UNICEF; WFP; WHO.

Hadgu, K.M., Kooistra, L., Rossing, W.A.H., van Bruggen, A.H.C., 2009. Assessing the effect of Faidherbia albida based land use systems on barley yield at field and regional scale in the highlands of Tigray, Northern Ethiopia. Food Secur. 1, 337–350. https://doi.org/10.1007/s12571-009-0030-2.

Harmand, J.-M., Njiti, C.F., 1992. Faidherbia albida in Northern Cameroon: provenance trials and crop associations. In: Foidherbia Albida in the West African Semi-Arid Tropics: Proceedings of a Workshop. ICRISAT-ICRAF, pp. 79–82.

Henning, R.J., Brown, R.H., Ashley, D.A., 1979. Effects of leaf position and plant age on photosynthesis and translocation in peanut I. Apparent photosynthesis and 14C translocation. Peanut Sci. 6, 46–50.

Hiemstra, P.H., Pebesma, E.J., Twenhöfel, C.J., Heuvelink, G.B., 2009. Real-time automatic interpolation of ambient gamma dose rates from the Dutch radioactivity monitoring network. Comput. Geosci. 35, 1711–1721.

Jayne, T.S., Fox, L., Fuglie, K., Adelaja, A., 2021. Agricultural Productivity Growth, Resilience, and Economic Transformation in Sub-Saharan Africa. Association of Public and Land-grant Universities (APLU).

Jung, J., 1970. Seasonal variations in the microbiological characteristics of a weakly leached, tropical ferruginous soil (DIOR), with or without the influence of Acacia albida. Oecologia Plant. 5, 113–135.

Karlson, M., Bolin, D., Bazié, H.R., Ouedraogo, A.S., Soro, B., Sanou, J., Bayala, J., Ostwald, M., 2023. Exploring the landscape scale influences of tree cover on crop yield in an agroforestry parkland using satellite data and spatial statistics. J. Arid Environ. 218, 105051. https://doi.org/10.1016/j.jaridenv.2023.105051.

Kho, R.M., Yacouba, B., Yaye, M., Katkore, B., Moussa, A., Iktam, A., Mayaki, A., 2001. Separating the effects of trees on crops: the case of faidherbia albida and millet in Niger. Agrofor. Syst. 52, 219–238. https://doi.org/10.1023/a:1011820412140.

Kuhn, M., 2008. Building predictive models in R using the caret package. J. Stat. Softw. 28, 1–26. https://doi.org/10.18637/jss.v028.i05.

Leroux, L., Falconnier, G.N., Diouf, A.A., Ndao, B., Gbodjo, J.E., Tall, L., Balde, A.A., Clermont-Dauphin, C., Bégué, A., Affholder, F., Roupsard, O., 2020. Using remote sensing to assess the effect of trees on millet yield in complex parklands of central Senegal. Agric. Syst. 184, 102918. https://doi.org/10.1016/j.agsy.2020.102918.

Leroux, L., Clermont-Dauphin, C., Ndienor, M., Jourdan, C., Roupsard, O., Seghieri, J., 2022. A spatialized assessment of ecosystem service relationships in a multifunctional agroforestry landscape of Senegal. Sci. Total Environ. 853, 158707. https://doi.org/10.1016/j.scitotenv.2022.158707.

Louppe, D., N'dour, B., Samba, S.A.N., 1996. Influence de faidherbia albida sur l'arachide et le mil au Sénégal: Méthodologie de mesure et estimations des effets d'arbre émondés avec ou sans parcage d'animaux. In: Les parcs à Faidherbia. Cahiers scientifiques, pp. 123–139.

Matérn, B., 1960. Spatial variation. Stochastic models and their application to some problems in forest surveys and other sampling investigations.

Matos, F.S., Wolfgramm, R., Gonçalves, F.V., Cavatte, P.C., Ventrella, M.C., DaMatta, F. M., 2009. Phenotypic plasticity in response to light in the coffee tree. Environ. Exp. Bot. 67, 421–427.

Mbow, C., Van Noordwijk, M., Luedeling, E., Neufeldt, H., Minang, P.A., Kowero, G., 2014. Agroforestry solutions to address food security and climate change challenges in Africa. Curr. Opin. Environ. Sustain. 6, 61–67.

Mead, R., Willey, R.W., 1980. The concept of a 'land equivalent ratio' and advantages in yields from intercropping. Exp. Agric. 16, 217–228. https://doi.org/10.1017/S0014479700010978.

Noba, K., Ngom, A., Guèye, M., Bassène, C., Kane, M., Diop, I., Ndoye, F., Mbaye, M.S., Kane, A., Ba, A.T., 2014. L'arachide au Sénégal: état des lieux, contraintes et perspectives pour la relance de la filière. OCL 21, D205. https://doi.org/10.1051/ocl/2013039.

Olatinwo, R., Hoogenboom, G., 2014. Chapter 4 – weather-based pest forecasting for efficient crop protection. In: Abrol, D.P. (Ed.), Integrated Pest Management. Academic Press, San Diego, pp. 59–78. https://doi.org/10.1016/B978-0-12-398529-3.00005-1.

Pebesma, E.J., 2004. Multivariable geostatistics in S: the gstat package. Comput. Geosci. 30, 683–691.

Poschen, P., 1986. An evaluation of the acacia albida-based agroforestry practices in the hararghe highlands of eastern Ethiopia. Agrofor. Syst. 4, 129–143. https://doi.org/10.1007/BF00141545.

QGIS_Development_Team, 2019. QGIS Geographic Information System. Open Source Geospatial Foundation Project. ⟨http://qgis.osgeo.org⟩ ([WWW Document].

R Core Team, 2019. R: A Language and Environment for Statistical Computing, Version 3.6.1. R Foundation for Statistical Computing, Vienna, Austria. ⟨https://www.R-project.org/⟩.

Roupsard, O., Audebert, A., Ndour, A.P., Clermont-Dauphin, C., Agbohessou, Y., Sanou, J., Koala, J., Faye, E., Sambakhe, D., Jourdan, C., le Maire, G., Tall, L., Sanogo, D., Seghieri, J., Cournac, L., Leroux, L., 2020. How far does the tree affect the crop in agroforestry? New spatial analysis methods in a Faidherbia parkland. Agric. Ecosyst. Environ. 296, 106928. https://doi.org/10.1016/j.agee.2020.106928.

Rouse, J., Haas, R.H., Schell, J.A., Deering, D.W., 1974. Monitoring vegetation systems in the Great Plains with ERTS.

Sida, T.S., Baudron, F., Kim, H., Giller, K.E., 2018. Climate-smart agroforestry: Faidherbia albida trees buffer wheat against climatic extremes in the central rift valley of Ethiopia. Agric. For. Meteorol. 248, 339–347. https://doi.org/10.1016/j.agrformet.2017.10.013.

Sida, T.S., Baudron, F., Ndoli, A., Tirfessa, D., Giller, K.E., 2019. Should fertilizer recommendations be adapted to parkland agroforestry systems? Case studies from Ethiopia and Rwanda. Plant Soil 1–16.

Siegwart, L., Bertrand, I., Roupsard, O., Jourdan, C., 2023. Contribution of tree and crop roots to soil carbon stocks in a sub-Sahelian agroforestry parkland in Senegal. Agric. Ecosyst. Environ. 352, 108524. https://doi.org/10.1016/j.agee.2023.108524.

Singh, A., 2003. Phenology of Groundnut, pp. 295–382.

Stein, M.L., 2012. Interpolation of Spatial Data: Some Theory for Kriging. Springer Science & Business Media.

Tang, L., Shao, G., 2015. Drone remote sensing for forestry research and practices. J. For. Res. 26, 791–797. https://doi.org/10.1007/s11676-015-0088-y.

Tomlinson, H., Traore, A., Teklehaimanot, Z., 1998. An investigation of the root distribution of Parkia biglobosa in Burkina Faso, West Africa, using a logarithmic spiral trench. For. Ecol. Manag. 107, 173–182.

Umar, B.B., Aune, J.B., Lungu, O.I., 2013. Effects of Faidherbia albida on the fertility of soil in smallholder conservation agriculture systems in eastern and Southern Zambia. Afr. J. Agric. Res. 8, 173–183. https://doi.org/10.5897/AJAR11.2464.

Van Leeuwen, W.J.D., Huete, A.R., 1996. Effects of standing litter on the biophysical interpretation of plant canopies with spectral indices. Remote Sens. Environ. 55, 123–138. https://doi.org/10.1016/0034-4257(95)00198-0.

Wudil, A.H., Usman, M., Rosak-Szyrocka, J., Pilař, L., Boye, M., 2022. Reversing years for global food security: a review of the food security situation in sub-Saharan Africa (SSA). Int. J. Environ. Res. Public Health 19, 14836. https://doi.org/10.3390/ijerph192214836.

Yengwe, J., Amalia, O., Lungu, O.I., De Neve, S., 2018. Quantifying nutrient deposition and yield levels of maize (Zea mays) under Faidherbia albida agroforestry system in Zambia. Eur. J. Agron. 99, 148–155.

Zongo, A., Konate, A.K., Koïta, K., Sawadogo, M., Sankara, P., Ntare, B.R., Desmae, H., 2019. Diallel analysis of early leaf spot (Cercospora arachidicola Hori) disease resistance in groundnut. Agronomy 9, 15. https://doi.org/10.3390/agronomy9010015.